Journal of Archaeological Science 149 (2023) 105695

Contents lists available at ScienceDirect

Journal of Archaeological Science

journal homepage: www.elsevier.com/locate/jas

A large-scale Sr and Nd isotope baseline for archaeological provenance in Silk Road regions and its application to plant-ash glass

Qin-Qin Lü [a,b,*], Yi-Xiang Chen [c,d], Julian Henderson [e], Germain Bayon [f]

[a] Department for the History of Science and Scientific Archaeology, University of Science and Technology of China, Hefei, 230026, China
[b] McDonald Institute for Archaeological Research, University of Cambridge, Cambridge, CB2 3ER, UK
[c] CAS Key Laboratory of Crust-Mantle Materials and Environments, School of Earth and Space Sciences, University of Science and Technology of China, Hefei, 230026, China
[d] CAS Center for Excellence in Comparative Planetology, University of Science and Technology of China, Hefei, 230026, China
[e] Department of Classics and Archaeology, University of Nottingham, University Park, Nottingham, NG7 2RD, UK
[f] Univ Brest, CNRS, Ifremer, Geo-Ocean, Plouzané, F-29280, France

ARTICLE INFO

Keywords:
Bioavailable Sr isotopes
Detrital Nd isotopes
Archaeological provenance
Plant-ash glass
Silk Roads
Central Asia
West Asia

ABSTRACT

Bioavailable Sr and detrital Nd isotopes are important tools for archaeological provenance. To apply Sr and Nd isotopes for provenance, regional isotope databases and baselines are generally needed. For the vast Silk Road regions of Mesopotamia, Iran, and Central Asia, detailed isotopic distribution patterns essential for determining provenance may not become available in the short term due to the severe deficiency of available data. In the present work, we investigate the geo-environmental factors controlling the Sr and Nd isotopic signatures and use published data from archaeology and Earth sciences, selected by rigorous criteria, to construct the first large-scale, semi-quantitative Sr–Nd isotope baseline for these Silk Road regions. Three isotopic zones are proposed for Central Asia: CA-1 (mountains), $\varepsilon_{Nd} < -7.5$, $^{87}Sr/^{86}Sr > 0.7095$; CA-2 (deserts), $\varepsilon_{Nd} = -5$ to -2, $^{87}Sr/^{86}Sr \sim 0.709$; CA-3 (loess), $\varepsilon_{Nd} = -5$ to -2, $^{87}Sr/^{86}Sr > 0.710$. General isotopic signatures are suggested for Iran: $\varepsilon_{Nd} = -8$ to -4, $^{87}Sr/^{86}Sr = 0.7075$–0.7090. Three isotopic zones are proposed for Mesopotamia: MP-1 (floodplain and foothill), $\varepsilon_{Nd} = -6.5$ to -4 (putative extended range MP-1N, $\varepsilon_{Nd} = -8$ to -6), $^{87}Sr/^{86}Sr = 0.7080$–0.7085; MP-2 (deserts), $\varepsilon_{Nd} < -8$, $^{87}Sr/^{86}Sr > 0.7085$; MP-3 (Syrian Euphrates), $\varepsilon_{Nd} = -5.5$ to -2, $^{87}Sr/^{86}Sr = 0.7080$–0.7085. Within the limitation of available data, these ranges indicate the overall trend of bioavailable Sr and detrital Nd isotopic signatures for each isotopic zone, which are controlled by their geological context, climate (e.g., precipitation), and various Earth surface processes (e.g., riverine versus aeolian transport). This baseline can be used as an essential guide for geochemical contexts to suggest or verify the provenance of plant-ash glass, serving as part of an integrative Sr–Nd isotopic approach. We illustrate the potential of this approach using two case studies. By investigating the isotopic compositions of Mesopotamian plant-ash glass, we suggest possible northern Mesopotamian origins for plant ash and silica raw materials used for Mesopotamian glass-making. By reassessing medieval plant-ash glass from San Lorenzo, Italy, we propose diverse origins including Central Asia and Mesopotamia. Additionally, as part of this isotopic approach, by examining the Nd isotope mixing lines in the context provided by the Nd isotope baseline, we reveal the occurrence of glass recycling for Islamic plant-ash glass from different production zones in association with a westward spread from Mesopotamia to the Eastern Mediterranean metropolises.

1. Introduction

Radiogenic Sr and Nd isotopes are among the most commonly used isotopic tools in Earth sciences. Initially used for geochronological purposes, they have become indispensable in the study of geological processes from the deep Earth to surface environments. Sr and Nd isotopic analyses are based on the respective decay of radioactive isotopes ^{87}Rb and ^{147}Sm into radiogenic isotopes ^{87}Sr and ^{143}Nd. The relative abundances of radiogenic isotopes in geological samples, expressed using the $^{87}Sr/^{86}Sr$ and $^{143}Nd/^{144}Nd$ ratios, are set by the initial parent-

* Corresponding author. Department for the History of Science and Scientific Archaeology, University of Science and Technology of China, Hefei 230026, China.
E-mail address: qinqinlu@icloud.com (Q.-Q. Lü).

https://doi.org/10.1016/j.jas.2022.105695
Received 12 December 2021; Received in revised form 26 October 2022; Accepted 27 October 2022
Available online 14 November 2022

daughter compositions and the elapsed geologic time. In general, mantle-derived, younger, mafic rocks tend to exhibit relatively low $^{87}Sr/^{86}Sr$ and high $^{143}Nd/^{144}Nd$ ratios, while crust-derived, older, felsic rocks usually possess high $^{87}Sr/^{86}Sr$ and low $^{143}Nd/^{144}Nd$ ratios (White and Hofmann, 1982). Because of their role in geochemical fingerprinting, Sr and Nd isotopes are particularly useful for source tracing and have been employed as tracers in a wide range of surface processes, such as tracking the source of transported sediments, provenancing desert sands and dust, and tracing the circulation of oceanic currents (e.g., Banner, 2004; Frank, 2002; Goldstein and Jacobsen, 1988; Goldstein et al., 1984; Grousset and Biscaye, 2005).

Sr and Nd isotopes are applicable to archaeological provenance studies because archaeological samples are made of materials that are ultimately derived from geological and ecological processes. Sr isotopes have been extensively used for ancient diet reconstruction and human/faunal mobility studies (e.g., Beard and Johnson, 2000; Bentley, 2006; Ericson, 1985; Price et al., 1994, 2002). Sr and Nd isotopes (sometimes in combination with Pb isotopes) have been applied to trace the origin of ceramics (e.g., Carter et al., 2011; De Bonis et al., 2018; Li et al., 2006, 2005; Zhang et al., 2004). Importantly, Sr and Nd isotopes have been proven beneficial for plant-ash glass provenance (e.g., Brill and Fullagar, 2009; Degryse et al., 2010a, 2010b; Freestone et al., 2003; Freestone, 2006; Henderson et al., 2005, 2010) and natron glass provenance (e.g., Degryse and Schneider, 2008; Freestone et al., 2003; Ganio et al., 2012; Henderson et al., 2005; Wedepohl and Baumann, 2000). The use of Sr and Nd isotopes for plant-ash glass provenance is noteworthy. Current research has reported the isotopic signatures of plant-ash glasses produced in Late Bronze Age (LBA) Egypt and Mesopotamia, southeastern Arabia (1st century), Iraq (Sasanian period), and the Islamic Levant and Syria. For the LBA and the Islamic period, by comparing isotopic compositions of glasses from different sites and of possible raw materials, researchers have proposed independent glass-making in the Eastern Mediterranean and Mesopotamia (Degryse et al., 2010a, 2010b, 2015; Freestone et al., 2003; Ganio et al., 2013; Henderson et al., 2005, 2009, 2010).

For archaeological provenance, the interpretation of Sr and Nd isotopes varies and depends on the types of samples under investigation. For instance, $^{87}Sr/^{86}Sr$ ratios in human and faunal tooth enamel reflect the water and dietary intake (Bentley, 2006), and measured $^{87}Sr/^{86}Sr$ ratios in plant-ash glass are inherited from the ashed halophytic plants used as flux in glass-making (Freestone et al., 2003). The Sr contents in these samples have a biological origin, thus, the Sr isotopic composition should be consistent with the local bioavailable Sr isotopic range. Meanwhile, for natron glass, if the Sr contents were mainly introduced by the aragonite-rich coastal sand used for glass-making, its $^{87}Sr/^{86}Sr$ composition should reflect that of seawater (Freestone et al., 2003), and other lime sources in the sand and the addition of limestone can also affect the Sr isotopic composition of natron glass. For Nd isotopes, the Nd budget and corresponding $^{143}Nd/^{144}Nd$ composition of archaeological glass are controlled by vitrifying materials such as quartz sand (Degryse and Schneider, 2008). Meanwhile, for pottery, the Nd contents derive mostly from clay and temper sources. Therefore, for provenancing glass and ceramics, the Nd isotopic signatures associated with regional clastic sediments (sand, gravel, clay, silt, etc.) are more relevant (referred to as 'detrital Nd').

Provenance studies typically require a reference database that can be used for comparison purposes. Unfortunately, available Sr–Nd isotopic data are still lacking in many regions. This is the case for the large area extending from Mesopotamia to Central Asia, which has a large spectrum of geo-environmental conditions and an immensely rich cultural heritage. This region was crucial for the communications and exchanges on the Silk Roads. However, to date, this area has been geochemically and archaeologically understudied. Considering the cost of sampling and analysis, the low density of data in this large region is not expected to be improved in the short term. This situation is especially true for plant-ash glass research. Existing chemical and isotopic analyses have mainly focused on the Eastern Mediterranean. Meanwhile, isotope data of plant-ash glass and glass-making materials from Mesopotamia are currently limited, and to our knowledge, no glass-related Sr and Nd isotopic analyses have been formally reported from Iran and Central Asia (except for the mention of Sr isotope results in Brill and Fullagar, 2009). Without previously accumulated data for comparison, the potential of newly reported data cannot be fully exploited. For example, although Sasanian glass from Veh Ardashir, Iraq was studied with Nd and Sr isotopes (Ganio et al., 2013), the specific provenance of the glass was not suggested since no isotopic compositions of raw materials or comparable glass samples were available.

In the absence of an extensive reference database, identifying the general compositional variability of the regions under investigation represents a first step toward successful provenance determination. As already shown by metal provenance studies using lead isotopes, if large-scale Pb isotopic signatures are known for the regions, a geologically-informed inference about metal provenance can be made in the absence of isotope data from individual reference ores (Albarède et al., 2012; Artioli et al., 2020). When provenancing biological materials using Sr isotopes, even if a specific area of origin cannot be identified, eliminating the possibility of certain areas is still beneficial for provenance (Holt et al., 2021). Also, based on large-scale geologic histories of Pb ore formation, regions with ore deposits bearing indistinguishable Pb isotopic compositions can be indicated (Killick et al., 2020). These provenance studies using various isotope systems evidently show that a consideration of large-scale isotopic properties can significantly inform future research.

In the present work, we attempt to construct a general Sr–Nd isotope framework for archaeological provenance in the regions of Mesopotamia, Iran, and Central Asia to partly alleviate the current lack of a reference database. We investigate the geological and environmental factors affecting the isotopic signatures, and compile published bioavailable Sr and detrital Nd isotope data from archaeological and environmental samples that fit our selection criteria. Rather than finding exact isotopic values, we propose major isotopic zones and the likely isotopic compositional ranges of each zone. The validity of this semi-quantitative Sr–Nd isotope baseline is confirmed in the two case studies that follow.

We also propose an integrative isotope approach for plant-ash glass provenance that is based on four pillars: chemical composition, Sr and Nd isotopic compositions, isotope mixing lines, and Sr–Nd isotope baseline. Chemical and Sr–Nd isotopic compositions are used to categorize glass artifacts into clusters that may indicate similar origins, as have been widely applied in current glass provenance works. Isotope mixing lines may suggest the occurrence of recycled glass and help explain compositional clustering results. The regional isotope baseline places compositional clusters into a geo-environmental context essential for verifying the sources of raw materials and the origin of glass. By seeking corroboration from the four lines of evidence, the best understanding of glass production and dispersion can be obtained. Using case studies of plant-ash glasses excavated from Mesopotamia and Italy, we demonstrate the benefit of using the Sr–Nd isotope baseline and this integrative approach for plant-ash glass provenance.

2. Method

2.1. Description

It is worthwhile to first look at how isotope baselines have been established in other regions. There have been considerable efforts to build quantitative regional isotope baselines ('isoscapes'), usually by processing a large amount of data from direct sampling. For example, many of the bioavailable Sr isotope maps are based on spatially dense empirical data (e.g., Blank et al., 2018; Evans et al., 2010; Frei and Frei, 2011; Hartman and Richards, 2014; James et al., 2022; Ladegaard-Pedersen et al., 2020; Laffoon et al., 2012 Nafplioti, 2011; Scaffidi and

Knudson, 2020; Snoeck et al., 2020; Wang et al., 2018; Wang and Tang, 2020; Willmes et al., 2018, 2014). An alternative approach is to predict $^{87}Sr/^{86}Sr$ ratios by leveraging geochemical and environmental knowledge about bedrock age and lithology as well as chemical weathering (Bataille et al., 2014; Bataille and Bowen, 2012; Beard and Johnson, 2000; Hegg et al., 2013). However, accurate mechanistic modeling of complex Earth surface processes on a large spatial scale often poses serious challenges. Consequently, bioavailable Sr isoscapes that statistically incorporate empirical data and geo-environmental covariates have been under development (e.g., Bataille et al., 2020, 2018; Brennan et al., 2016; Janzen et al., 2020; Serna et al., 2020).

In contrast, there has been relatively less focus on Nd isotope baselines, although Nd isotope data of terrestrial surface rocks have been aggregated (e.g., the compilations by Blanchet, 2019; Jeandel et al., 2007; Robinson et al., 2021, and EarthChem http://portal.earthchem.org/) and can be used for sediment provenance. Compared to Sr isotope databases, Nd isotope databases have been developed more recently and have smaller coverages (Banner, 2004). Furthermore, unlike radiogenic Sr, which displays a uniform isotopic composition in seawater at a given point in geologic time (e.g., modern seawater $^{87}Sr/^{86}Sr = 0.709179$, Mokadem et al., 2015), Nd isotopic ratios exhibit a large variability in seawater due to a much shorter oceanic residence time (Lacan et al., 2012; Tachikawa et al., 2017), and a single global Nd isotope signal did not exist (Banner, 2004).

Establishing a quantitative baseline requires both systematic sampling and prior geological knowledge. In empirical studies of bioavailable Sr isoscapes, a geologic map is usually needed to guide the choice of sampling locations, and lithological grouping is commonly used as a useful constraint. On the other hand, the results of *ab initio* modeling need to be examined against empirical data to verify the model's predictability. In fact, an isoscape's potential to predict generally relies on geologic understanding and the density of data, both of which need to positively correlate with the complexity of regional geology (e.g., see case studies in Bataille et al., 2020). However, if detailed geologic surveys and environmental monitoring have not been conducted in a region and available isotope data are scarce or nonexistent, then neither geologically-informed models nor the interpolation of data points would have a prediction power larger than qualitative research.

To trace the origins of archaeological samples in areas with limited data, we need an approach that fully harnesses the information at our disposal. This approach should take heed of the underlying geological and environmental background and investigate the major controls of isotopic compositions. This would help demarcate the region into major geo-environmental groups (or isotopic zones), thereby accounting for the most general spatial variations. On top of this qualitative zoning, available empirical data can be used to *anchor* the representative isotopic value of each identified isotopic zone, although the exact isotopic ranges of these zones will be determined by future reported data. In this way, the established semi-quantitative baseline is still built on both actual data and geological/environmental knowledge. In essence, this is somewhat analogous to the domain mapping method of isoscape construction that was used in previous studies on bioavailable Sr isoscapes (e.g., Evans et al., 2010; Hodell et al., 2004; Ladegaard-Pedersen et al., 2020; Snoeck et al., 2020). The domain mapping approach links data (or data clusters) to geographical groups with similar lithology, and is best used for areas with homogeneous, well-understood lithological conditions and where superficial deposits do not significantly deviate from bedrock geology (Holt et al., 2021). In the present study, we attempt to relate both Sr and Nd isotope data to specific areas while considering not only the underlying lithologies but also exogenous (such as riverine and atmospheric) inputs. Although our data are not acquired from proactive sampling, which is impractical at this stage, we set rigorous criteria for selecting published data with the aim of archaeological provenance.

Finally, another subtlety about sampling arises from the nature of archaeology. In the provenance of synthesized ancient material culture, the artifact to be provenanced is compared to raw ingredients possibly used to make it. Preferably, we should compare excavated ancient material culture with raw ingredients occurring near production centers and known to be relevant to ancient production activities. However, this is usually rather impractical. For instance, historical records of glass production or direct archaeological evidence for glass-making are lacking in many regions. As a result, scientists have conducted large-scale surveys of possible raw materials in the hope of narrowing the range of sources for provenance. Such examples include the investigation of the isotopic compositions of Syrian and Lebanese plants and sands for plant-ash glass provenance (Henderson et al., 2009, 2020b), and the search using chemical and Sr–Nd isotopic compositions for beach sands suitable for Roman glass-making (Brems et al., 2012, 2013a, 2013b). These studies show that, with well-defined sample selection and/or data screening strategies, the consideration of environmental samples from a large geographical range can inform the search for possible raw materials and help provenance material culture.

2.2. Data compilation

We assembled bioavailable Sr and detrital Nd isotope data from existing archaeological and geoscience publications. The sampling locations are displayed against the background of general bedrock geology in Fig. 1. The Sr isotopes are reported using the $^{87}Sr/^{86}Sr$ ratio, and the Nd isotopes are expressed using the conventional ε_{Nd} notation:

$$\varepsilon_{Nd} = \left[\frac{\left(^{143}Nd/^{144}Nd\right)_{sample}}{\left(^{143}Nd/^{144}Nd\right)_{CHUR}} - 1\right] \times 10^4$$

where $(^{143}Nd/^{144}Nd)_{CHUR} = 0.512638$. Note that all data used in this study have been normalized to the same $(^{143}Nd/^{144}Nd)_{CHUR}$ value. The ε_{Nd} parameter denotes the extent to which the sample's Nd isotope ratio deviates from the present-day value of the Chondritic Uniform Reservoir (CHUR) (Jacobsen and Wasserburg, 1980).

For provenance studies using isotopes, it is paramount to use geologically screened data whose geologic significance has been carefully assessed (Artioli et al., 2020). Our data selection criteria are explained as follows. We focused on data from surface features and neglected geology deeper than near-surface. Because we are mainly concerned with large-scale trends among the regions, we prefer data representing average values for large areas when such data are available.

Sr is a mobile element that is preferentially leached from rocks during chemical weathering and erosional processes. The exchangeable (i.e., bioavailable) Sr fraction entering the hydrosphere is dominated by preferential dissolution of easily altered rocks (such as carbonates and evaporates) or rock-forming minerals (such as apatite and plagioclase), which are commonly enriched in Sr (e.g., Aubert et al., 2001; Capo et al., 1998). In addition, atmospheric inputs in the form of wet (rainfall, sea spray) and dry (aeolian dust) deposition, glacial deposition, and agricultural fertilizers also contribute to the exchangeable Sr pool in soils (e.g., Capo et al., 1998; Hartman and Richards, 2014; Holt et al., 2021; Pett-Ridge et al., 2009; Hedman et al., 2009). Therefore, despite major influence from the substrate, the bioavailable $^{87}Sr/^{86}Sr$ in soils (and by extension, the terrestrial biosphere) does not exactly mirror the bedrock's isotopic value (Bentley, 2006), and substantial disparities in Sr isotopes among whole rocks, bulk soil, and the exchangeable fraction in soils may occur (Bataille et al., 2020; Sillen et al., 1998). The labile Sr in soils is taken up by plants and enters the food chain. However, we did not include soil leachates in the data used for baseline construction since they are usually very variable and may yield values inconsistent with plants (Evans and Tatham, 2004; Maurer et al., 2012; Ryan et al., 2018). We have, however, included results from surface water (but not groundwater), such as rivers and lakes, as suggested by existing research (e.g., Evans et al., 2010; Frei and Frei, 2011; Ladegaard-Pedersen et al., 2020; Maurer et al., 2012; Wang et al., 2018). Surface water reflects the average Sr isotopic composition of large catchment areas, serving as an

Fig. 1. (Color online) Map of Mesopotamia, Iran, and Central Asia showing simplified bedrock geology, sampling or excavated locations (sample types of vegetation, water, faunal or human samples for Sr isotopes, and surficial or riverine detrital sediments for Nd isotopes, and plant-ash glass), and major ancient cities. The map was created with QGIS (https://www.qgis.org/) by adapting two overlaid layers: *CGMW Bedrock and Structural Geology* and *Natural Earth II with Shaded Relief, Water, and Drainages*.

easy-to-obtain signal to characterize the watershed when more extensive sampling is absent. When spatially dense sampling becomes available, data from large water bodies may be replaced but can still function as useful references.

Because measured radiogenic isotopes are systematically normalized to a given stable isotope ratio during analysis (for instance using $^{86}Sr/^{88}Sr = 0.1194$), reported $^{87}Sr/^{86}Sr$ values in the literature are not determined by natural mass-dependent fractionation related to biological or Earth surface processes. This implies that measured Sr isotopic compositions for plant or animal samples faithfully correspond to local bioavailable $^{87}Sr/^{86}Sr$ signatures, e.g., as shown by relatively consistent $^{87}Sr/^{86}Sr$ ratios transferred up the food chain (Blum et al., 2000), except for those samples that cannot be linked to any specific regional habitat, such as migratory animals. Vegetation is one of the recommended archives for constructing Sr isoscapes since it is widely available and directly represents the strontium that enters the food chain at a specific locality (e.g., Evans et al., 2010, 2009; Evans and Tatham, 2004; Holt et al., 2021; Maurer et al., 2012; Snoeck et al., 2020; Willmes et al., 2018). A single plant may exhibit unrepresentative values if it absorbs Sr from a confined or discrete cation pool, thus, the collection and combination of multiple plants from near the same sampling point ('homogenized sampling') are suggested to reduce the effect of extremely localized biases (Holt et al., 2021). Here, to construct Sr baselines, we ensured that for plant data, each data point contains multiple plant samples. Small, low-mobility animals have also been advocated as a good choice of samples to represent the local bioavailable $^{87}Sr/^{86}Sr$ since they have a local feeding range (Price et al., 2002). Gathering animal samples was not feasible for us, so we have included in the dataset archaeological human and faunal samples. The data used are from archaeologically excavated tooth enamels and eggshells (from ostrich, a flightless bird). Ostrich shells from Mesopotamia have been tentatively included considering the mention of ostrich exploitation in Assyrian texts (Hodos et al., 2020) and that they generally match other data from the region. Data from bones were not chosen because bones typically undergo remodeling throughout the individual's lifespan and are also prone to diagenetic contamination (Bentley, 2006; Hoppe et al., 2003; Koch et al., 1997; Price et al., 2002). We did not use data from snails because they are often biased toward the values of rainwater and carbonates (Evans et al., 2010). To ensure the local origins of archaeological samples, we excluded any data that were indicated in the source publications as immigrants or having nonlocal origins. Normally, Sr isotope data from modern humans should not be used for archaeological provenance due to their increased mobility and dietary variety. We have, however, included data from modern Iranians and one modern Afghan individual as secondary evidence because there are no or very few data reported from these regions. Due to changes in environmental conditions over the geologic timescale, fossils are not used as data sources.

In particular, to provenance plant-ash glass, we are most concerned with the Sr isotopic compositions of plants. In mobility studies, plant samples are typically used to derive a range that interprets the origin of animals or humans. Here, we explain the motivation behind using excavated faunal and human samples to provenance plant-ash glass. Since animals acquire their Sr isotopic signatures from averaging their food intake, they have been observed to possess $^{87}Sr/^{86}Sr$ ratios that are less variable than the plants they consume, thus, faunal samples should provide a conservative constraint for the local biome (Price et al., 2002). In other words, faunal/human samples can inform, in an average sense, the overall trend of the local plants' isotopic compositions (Holt et al., 2021) and, by extension, the isotopic composition of plant-ash glass. In this context, whether the $^{87}Sr/^{86}Sr$ ratio of a specific glass artifact is slightly outside the range given by faunal/human samples is less important since we only need to provide an anchor for bioavailable $^{87}Sr/^{86}Sr$ ranges instead of obtaining the full range.

Applying Nd isotopes for provenancing archaeological materials such as glass and ceramics is largely analogous to using them for sediment provenance. The Sm and Nd contents in these archaeological materials are typically associated with REE-bearing accessory minerals (e.g., monazite, allanite, apatite, titanite, zircon) and some of the rock-forming minerals (e.g., feldspar, pyroxene), and these minerals are contained in detrital particles as raw ingredients derived from the erosion of crustal rocks (Bayon et al., 2015; Brems et al., 2013b). For siliciclastic sediments, chemical weathering and mineral sorting during sediment transport generally result in negligible Nd isotope decoupling (Bayon et al., 2015; Meyer et al., 2011). The Nd isotope ratio, therefore, acts as a robust provenance proxy that is generally unaffected by Earth surface processes and preserves the primary isotopic signature of the source area (Banner, 2004; Bayon et al., 2015; Degryse and Schneider, 2008; Grousset and Biscaye, 2005). Therefore, reported Nd isotopic analyses for surface detrital sediment can generally be used as reliable local Nd isotopic signatures in archaeological provenance studies. Here, we have included data from riverine and wetland sediments, desert sand, soil, and the top surface of drilled sediment cores. Data from ore deposits are not used since they are irrelevant to the provenance of siliciclastic-sediment-based artifacts (e.g., glass and ceramics).

It is worth emphasizing that Nd isotopes in non-silicate components of sediments are not considered in this study. Marine precipitates such as carbonates are typically more radiogenic in Nd isotopes than the associated silicates and are also preferentially weathered (Faure and Mensing, 2005; Goldstein and Jacobsen, 1988; Hindshaw et al., 2018). Sedimentary Fe-oxides may display different ε_{Nd} signatures than detrital fractions (Bayon et al., 2020). Other non-terrigenous sediment phases (e.g., Fe–Mn oxyhydroxides and organic matter) may contain Nd as well (Bayon et al., 2002). It is therefore nontrivial to clarify that the Nd isotope data used here are specifically of the terrigenous fraction, i.e., the silicate residues after the organic and carbonate fractions have been removed by the leaching process. This implies that if a significant portion of the Nd contents in the archaeological material to be provenanced have a non-continental origin, this baseline may not fully apply.

We additionally discuss aeolian and riverine samples as archives for Sr and Nd isotopes. Aeolian deposition can be significant and may sometimes dominate the Sr and Nd budgets in the surface layer (Bataille et al., 2020; Hartman and Richards, 2014; Pett-Ridge et al., 2009; Weldeab et al., 2002). In dust, $^{87}Sr/^{86}Sr$ typically strongly increases as grain size decreases, indicating that it is sensitive to the effect of wind sorting, but the Nd isotope ratio does not vary much with grain size and is considered more pertinent to the dust origin (Feng et al., 2009). The sources of aeolian dust can be highly complex and are not necessarily local (see discussion in the online Supplementary Material – SM). Aeolian dust from exposed marine carbonates has a very different impact than that from siliciclastic sediments on the $^{87}Sr/^{86}Sr$ signature of the surface (Capo et al., 1998). Therefore, it is necessary to consider aeolian deposition as one of the controlling processes, but we do not recommend directly using isotopic compositions of dust to establish the local range.

River systems and other water bodies integrate the isotopic compositional variability of fluxes in their catchments, thus fitting our purpose of examining large-scale trends. Therefore, dissolved Sr and detrital sediment Nd in rivers and water bodies can be used to construct Sr and Nd isotope baselines on the premise that the geo-environmental conditions of the watershed are known. The weathering of carbonaceous and other marine-derived sedimentary rocks generally shifts $^{87}Sr/^{86}Sr$ in water bodies toward less radiogenic values (Bayon et al., 2021) and causes the dissolved load's ε_{Nd} value to differ from the suspended particulates (Bayon et al., 2015). The preferential weathering of volcanic rocks in the drainage basin can also lead to a positive ε_{Nd} offset for fine-grained sediments (Bayon et al., 2015) and a negative $^{87}Sr/^{86}Sr$ shift for dissolved cations (Voerkelius et al., 2010). In riverine sediments, the Sr isotopic composition of the fine detrital fraction may deviate toward more radiogenic levels compared to the coarse fraction, while Nd isotopes are not significantly dependent on grain size (Bayon et al., 2015, 2021).

We have compiled Sr isotope data (Clauer et al., 2000; Elliott et al., 2015; Gregoricka, 2013; Henderson et al., 2009; Hodos et al., 2020; Kenoyer et al., 2013; Kutterer and Uerpmann, 2017; Pokrovsky et al., 2017; Posey, 2011; Wang et al., 2018) in Table S1 and Nd isotope data (Bayon et al., 2015; Chen et al., 2007; Cullen et al., 2000; Henderson et al., 2020b; Kumar et al., 2020; Sharifi et al., 2018; Sirocko, 1994) in Table S2 in SM Section 1. Since the data are not from preplanned sampling, they are inevitably distributed unevenly. As an intuitive reference for our estimation of isotopic ranges, we have also summarized, in Tables S3 and S4 (SM Section 5), the distinct isotopic groups identified in three studies (bioavailable Sr isotopes for France, Willmes et al., 2018, and the Maya region, Hodell et al., 2004, and Nd isotopes of sediments in rivers with medium or small watershed sizes, Bayon et al., 2015).

3. Isotope baseline

We investigate the isotopic signatures for each region following the Silk Road route from east to west by surveying the tectonic, erosion, and transport controls that are at work. In the following, for Central Asia, Iran, and Mesopotamia, we describe corresponding isotopic zones and their respective approximate ranges for Nd and Sr isotopes. A detailed discussion of the characteristic geological/environmental conditions of each isotopic zone is given in SM Sections 2–4. The isotopic ranges are decided by considering published data (Table S1, Table S2, Fig. 2). In addition to these data, additional data as indirect or secondary evidence are occasionally mentioned in the following discussion. The results are given in Table 1 and Fig. 2. Since our intention is to look for broad characteristics rather than exact values, the upper and lower bounds of these estimated ranges are set arbitrarily.

3.1. Central Asia

The distribution patterns for bioavailable Sr and detrital Nd isotopes in Central Asia are mainly controlled by the combined effects of rock erosion, aeolian deposition, and river transport (see SM Section 2). Based on the observed variability in distinct geo-environmental conditions, Central Asia can be divided into three main isotopic zones. Zone 1

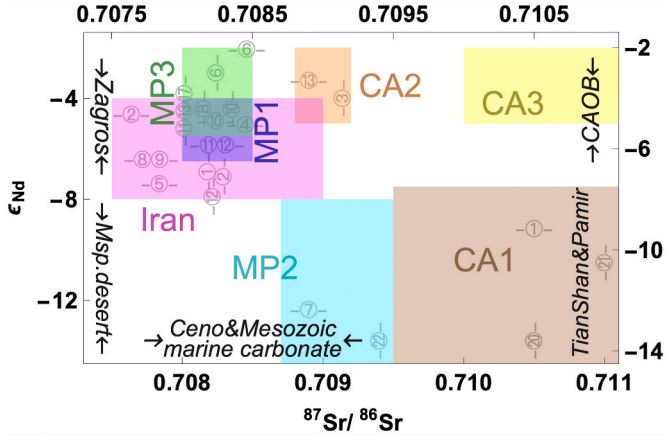

Fig. 2. (Color online) Estimated detrital ε_{Nd} and bioavailable $^{87}Sr/^{86}Sr$ ranges are displayed together with reported data (median value if consisting of multiple data) from environmental and bioarchaeological samples. The gray-colored circled numbers correspond to the data numbers in Tables S1–S2 (Section 1 in SM). The following isotopic zones are proposed: Central Asia (CA) 1–3, Iran, and Mesopotamia (MP) 1–3. Isotopic ranges of these zones are described in Table 1. Major geological features controlling the isotopic distribution patterns are indicated: Cenozoic & Mesozoic marine carbonate sediments, the Zagros, Mesopotamian deserts/semi-deserts, the CAOB, and the Tian Shan & Pamir Mountains. This illustration is only intended for indicating relations between the zones, and the ranges should not be taken as exact. See the text and the SM for data sources and details.

consists of mountainous areas including the Tian Shan and Pamirs, dominated by old continental rocks of Paleozoic and Precambrian ages. The glacier-fed rivers Amu Darya and Syr Dara may also exhibit isotopic signatures similar to those of Zone 1. Zone 2 includes deserts and sedimentary basins, which are mostly covered by Mesozoic and Cenozoic carbonaceous sedimentary rocks deposited in the Tethys and the Paratethys seas. Zone 3 is the piedmont loess in eastern Central Asia that resulted from aeolian deposition. Wind sorting is likely important in areas with significant aeolian deposition (Zones 2 and 3). Many locations of historical and archaeological significance, such as the Fergana Valley and Samarkand, are close to all three isotopic zones (Fig. 1).

Limited Nd and Sr isotope data have been reported for Central Asia. On a larger scale, siliciclastic materials of the massive Central Asian Orogenic Belt (CAOB) should overall have negative, relatively moderate ε_{Nd} values (such as several northern Chinese deserts in the CAOB with an average ε_{Nd} of −4.4, Li et al., 2011), but variations among blocks are expected to be significant. The ε_{Nd} values for deserts and loess in northern Central Asia may be comparable to sand in the nearby Gurbantunggut Desert in the Junggar Basin, northern Xinjiang, whose ε_{Nd} values were reported at −4.0 to −1.2 (Chen et al., 2007).

For the piedmont loess at the foot of mountains, because bioavailable Sr data are unavailable, soil in Kyrgyzstan from foothill locations such as Bishkek could be used as a strained reference, which has an average $^{87}Sr/^{86}Sr$ of 0.71579 (digested) (Dewan et al., 2015). The silicate component in the loess from the upper reaches of the Naryn River (a major tributary of the Syr Darya) was reported to have $^{87}Sr/^{86}Sr$ of approximately 0.720 (not bioavailable data) (Bujakaite et al., 2016). As a comparison, the mean $^{87}Sr/^{86}Sr$ of loess leachates in the Chinese Loess Plateau is 0.71122 (Wang and Tang, 2020).

For the Central Asian basins, the Aral Sea has been previously analyzed for $^{87}Sr/^{86}Sr$ in sediments (0.70992, Dewan et al., 2015) and in carbonates and water (both at 0.70914, Pokrovsky et al., 2017), and the latter value can be used as a regional bioavailable Sr signature for the sedimentary basin. The main source of exchangeable Sr in the Aral Basin is the Cretaceous–Paleogene calcareous strata derived from the Tethys and Paratethys sedimentary rocks (Pokrovsky et al., 2017), which should yield low $^{87}Sr/^{86}Sr$ ratios characteristic of seawater at that time (approximately 0.708, see Burke et al., 1982; McArthur et al., 2012). However, the weathering of silicate components brought by wind and rivers likely elevates the bioavailable $^{87}Sr/^{86}Sr$.

For the Central Asian mountains, reported Sr data from similar geologic zones in the vicinity are mentioned here as likely parallels: bioavailable $^{87}Sr/^{86}Sr$ is 0.7105 ± 0.0007 (1σ) for the Tian Shan and northern Tarim and 0.7110 ± 0.0009 (1σ) for the eastern Pamirs, both of which were reported from river waters on the Chinese side of the mountains (Wang et al., 2018). The riverine sediment from the final stretch of the Amu Darya in Uzbekistan has been analyzed: the $^{87}Sr/^{86}Sr$ ratio is 0.718455 for clay particles (not bioavailable data) (Bayon et al., 2021), and the ε_{Nd} value for the silt fractions is measured at −9.2 (Bayon et al., 2015), showing influence from mixed continental sources. Due to the efficient mixing of fine particles during riverine transport, the fine-grained sediment load in the lower course of rivers (or at the river mouth) provides integrated provenance information at the catchment scale. However, mountains often contribute significantly to the total Sr flux due to higher weathering rates at high altitudes and constant weathering of mountain-derived suspended particulates along the river's course (Bataille et al., 2020). The $^{87}Sr/^{86}Sr$ ratio of the Syr Darya water is 0.7094, indicating a strong influence from weathered silicates, and the $^{87}Sr/^{86}Sr$ ratio of the Amu Darya water is expected to be similar, if not higher, since both rivers are significantly affected by sediments from mountains and drain geologically comparable areas (Pokrovsky et al., 2017) and the Amu Darya may be especially prone to the influence of upstream detrital sediments (see Section 2 in SM). In addition, the Nd isotope ratios of the silicate fractions of cryoconites sampled from glaciers in the Tian Shan of Kyrgyzstan and the Pamir of Tajikistan range from −11.2 to −7.5 and −9.4 to −9.1, respectively, and the $^{87}Sr/^{86}Sr$

Table 1
Estimated detrital ε_{Nd} and bioavailable $^{87}Sr/^{86}Sr$ ranges.

Region	Isotopic zone	Zone description	ε_{Nd}	$^{87}Sr/^{86}Sr$	Main geo-environmental characteristics
Central Asia (CA)	Zone 1	mountains, Amu Darya, Syr Darya	< −7.5	>0.7095	Precambrian & Paleozoic crustal rocks, river transport
	Zone 2	deserts and sedimentary basins	−5 to −2	~0.709	Mesozoic & Cenozoic calcareous sediments, aeolian deposition
	Zone 3	loess	−5 to −2	>0.710	aeolian deposition
Iran	details unknown	plateau, mountains	−8 to −4	0.7075–0.7090	Mesozoic & Cenozoic calcareous sediments, mix of mafic and felsic rocks
Mesopotamia and environs (MP)	Zone 1	foothills, Tigris River, floodplain	−6.5 to −4 (putative Zone 1 N: −8 to −6)	0.7080–07085	river transport, fluvial deposition
	Zone 2	deserts, semi-deserts, and uplands	<-8	unknown, assumed >0.7085	aeolian deposition, erosion of Mesozoic & Paleozoic outcrops, Mesozoic & Cenozoic calcareous sediments
	Zone 3	Euphrates Valley (Syria)	−5.5 to −2	0.7080–07085	Cenozoic mafic formations, river transport

ratios of soluble, organic, and carbonate fractions in the cryoconites from the Tian Shan are all slightly above 0.710 (Nagatsuka et al., 2014). These values may result from relatively local sources, since long-distance aeolian transport is considered less significant in Central Asia mountains (Li et al., 2018).

Central Asia's southwestern corner may be associated with slightly lower isotopic values, as the $^{87}Sr/^{86}Sr$ ratio for the Kara-Bogaz-Gol Bay is 0.708153 (Clauer et al., 2000), although this value is affected by water inputs from the nearby Caspian Sea. Isotopic signatures similar to southern mountainous Central Asia may also apply to Afghanistan. It has been reported that $^{87}Sr/^{86}Sr$ is 0.70904 for modern human tooth enamel from Afghanistan (Posey, 2011). The ε_{Nd} for the dust from the Sistan Basin — which receives alluvial clasts from rivers originating in the Hindu Kush and traversing central Afghanistan — is estimated at −11.5 (Kumar et al., 2020).

Combining these reported analyses, we propose that Zone 1 may have relatively high bioavailable $^{87}Sr/^{86}Sr$ (more than 0.7095) and relatively low ε_{Nd} values (for instance, lower than −7.5). Zone 2 should show slightly lower $^{87}Sr/^{86}Sr$ (~0.709) and relatively high ε_{Nd} values (probably −2 to −5). Zone 3 may exhibit high $^{87}Sr/^{86}Sr$ (likely larger than 0.71) and relatively high ε_{Nd} values (probably −2 to −5). It has been previously observed that in areas dominated by silicate lithologies (e.g., mudstone, sandstone, gneiss, and granite), bioavailable $^{87}Sr/^{86}Sr$ ratios are typically more variable, while carbonate-dominant, lithologically homogeneous areas usually display a tight bioavailable $^{87}Sr/^{86}Sr$ range (Bataille et al., 2020; Evans et al., 2010). Additionally, Sr isotopic signatures in topographically varying areas are harder to predict than generally level areas (Evans et al., 2009). Consequently, we expect a more variable isotopic range for geochemically complex, high-relief areas such as Zone 1 compared to carbonate-rich, flat territories such as Zone 2.

3.2. Iran

Iran's highland landscape was formed as a consequence of the Cimmerian Orogeny and the Alpine-Himalayan Orogeny. Much of Iran is covered by Mesozoic and Cenozoic sediments, interspersed by old and young igneous outcrops including extrusive and intrusive rocks and ophiolites. We can theoretically divide Iran into four major zones on the grounds of geologic history: northern Iran, central Iran, western Iran (the Zagros Mountain), and southeastern Iran (see SM Section 3). Iran is dominated by arid and semi-arid climates. Considering the absence of major glacier systems and large rivers, bioavailable Sr and detrital Nd isotopic distribution patterns for each zone should be mostly controlled by relatively local surficial sediments, although all four zones are marked by complex and diverse lithologies. The Zagros and Alborz Mountains are among the regions receiving the highest precipitation in Iran and are expected to dominate the Sr and Nd isotopic patterns in western and northern Iran through rock erosion/weathering and river transport. Soils in Iran are generally highly calcareous, with calcium carbonate usually above 25% (Roozitalab et al., 2018).

Isotope data reported from Iran are extremely inadequate. Fine-grained river sediments of the Sefid Rud in northwestern Iran, which originates in the Zagros and flows out of the Alborz into the Caspian Sea, have been analyzed for sediment Nd isotopes, showing relatively radiogenic ε_{Nd} values ranging between −6.5 and −4.6 (Bayon et al., 2015; Tudryn et al., 2016), a result from integrating varied lithologies (see Table S4). Soil from Fars Province in southern Iran is characterized by a lower ε_{Nd} value of −7.4 (Kumar et al., 2020). Because the small rivers draining the Zagros carry clastic sediments to the Persian Gulf and the Gulf of Oman, the top surface of the sediment core extracted from the Gulf should roughly reflect the gross composition of rocks in the Zagros, which shows an ε_{Nd} range of −6.9 to −6.0 (Sirocko, 1994). The sand dunes in the northern UAE, which are close to the Zagros extension in northern Oman, have $\varepsilon_{Nd} = -5.3$ (Kumar et al., 2020). Notably, there is a significant lack of available data for central Iran.

There is only one site with faunal tooth enamel data publicly reported, which is Tepe Yahya ($^{87}Sr/^{86}Sr = 0.708132$(Q1)–0.708301(Q3)) in Kerman Province, southern Iran (Gregoricka, 2013). In northern Iran, the Sr isotope ratios from the Caspian Sea and the rivers discharging into the Caspian from its southern coast are 0.708183 and 0.708293, respectively (Clauer et al., 2000), although the value of the Caspian reflects all of its catchment (including outside Iran). Unpublished Sr isotope data of faunal samples from the Atrek River valley in Kopet Dagh, northern Iran also align with the low Sr isotopic signatures mentioned above (personal communication with Zihua Tang). Modern human tooth enamels from cities across Iran show a large variation, although most of the data center around the approximate range of 0.70809–0.70840 (Posey, 2011), which concurs with Tepe Yahya and the Caspian waters. In this dataset of modern humans, no significant variations exist among different cities. This could support an overall uniformity of low $^{87}Sr/^{86}Sr$ in Iran but could also result from a diverse diet for modern humans that smooths out contrasting isotopic values.

Currently available data from Iran do not allow for a delineation of distinct ranges for each zone. Nonetheless, we can use educated guesses to suggest Iran's most general isotopic signature. The bioavailable Sr isotopes in Iran most likely derive from the erosion of marine and continental deposits in surficial sediments. This most likely involve Mesozoic marine-derived carbonates, which should hence exhibit $^{87}Sr/^{86}Sr$ ratios between 0.707 and 0.708 (McArthur et al., 2012). Additional endmembers likely include Tertiary volcanic rocks (usually low in $^{87}Sr/^{86}Sr$) and the widely occurring Cenozoic/Mesozoic siliciclastic sediments (usually high in $^{87}Sr/^{86}Sr$). We therefore tentatively propose a bioavailable $^{87}Sr/^{86}Sr$ range of 0.7075–0.709. Estimating the Nd isotopic signature is even more challenging. The regional terrigenous source of Nd likely corresponds to a mixture of Cenozoic and Mesozoic silicate sediments and Tertiary volcanic rocks, meaning that the variability is potentially large. The reported ε_{Nd} values of surficial sediments

range between −8 and −4, which may be used to represent the approximate range of regional values, although this relatively stable range could also be a consequence of efficient sediment mixing by rivers or in soils from which our data come. It is possible that southern Iran is on the lower end of this ε_{Nd} range with the Zagros dominating the geology. Certainly, actual isotopic results from Iran may show local variations due to geological and/or environmental complexity. Nevertheless, if our estimates about Iran's overall isotopic ranges hold, Iran, in general, may actually show a broad uniformity, which could be attributed to the buffering effect of widely occurring calcareous contents in weathered rocks and soils for Sr isotopes, as well as a natural mix of felsic and mafic rocks that cancels out extreme Nd isotopic compositions. The absence of long-range transport (e.g., compared to Central Asia) may have also prevented distinct isotopic pools from being funneled and amplified.

3.3. Mesopotamia

Mesopotamia, meaning "between rivers", is the region in western Asia dominated by the Tigris-Euphrates river system. Here, we consider the isotopic background for Iraq and the adjacent areas of eastern Syria, Kuwait, and Khuzestan in Iran. In Mesopotamia, large rivers — mainly the Tigris and the Euphrates — as well as aeolian dust play important roles in controlling the regional distribution patterns of detrital Nd and bioavailable Sr (see SM Section 4). The Mesopotamian Plain, combined with the Persian Gulf, forms a large foreland basin to the southwest of the Zagros (Fouad, 2010). We propose that Mesopotamia and its environs can be divided into three distinct isotopic zones. Zone 1 consists of the areas of northeastern Iraq (an extension of the Zagros), most of the Tigris drainage, the Mesopotamian Floodplain in southern Iraq, as well as Kuwait and the Khuzestan Plain. This zone is subject to the influence of the Zagros geology either directly or indirectly (as conveyed by the Tigris and other rivers). Zone 2 is the deserts and semi-deserts in western Iraq and eastern Syria, where dust storms have a significant effect. Mesozoic and, to a lesser extent, Paleozoic outcrops can be found in this zone. Zone 3 is the section of the Euphrates Valley in northern Mesopotamia.

Mesopotamian sediments from the southern floodplain and wetland have been analyzed, which yield an ε_{Nd} range of −4.3 to −6.0 (Kumar et al., 2020; Sharifi et al., 2018) (for comparison, $\varepsilon_{Nd} = -5.5$ for the dust collected in Baghdad, Cullen et al., 2000). The ε_{Nd} value for Kuwait soil, reported as −5.1 (Kumar et al., 2020), also falls into this range. Sites in southern Iraq have reported faunal and human samples with $^{87}Sr/^{86}Sr$ close to or very slightly higher than 0.708 (Hodos et al., 2020; Kenoyer et al., 2013). These numbers are indeed comparable to data from Iran, but the ε_{Nd} values from the floodplain seem to be on the more radiogenic end of the Iranian Zagros. Most of northeastern Iraq is geologically analogous to the folded region of the Iranian Zagros and should bear similar isotopic signatures, and pre-Jurassic outcrops are present. We therefore propose that there could be a sub-zone (Zone MP-1N) in northeastern Iraq with slightly lower ε_{Nd} values than the Mesopotamian Plain. This is, however, mostly speculative at this stage without reported Nd isotope data. For Sr isotopes, only a small dataset of plants from a foothill location in Iraqi Kurdistan is available for northeastern Iraq (0.708031(Q1)–0.708152(Q3)) (Elliott et al., 2015), which is comparable to southern Iraq. The Sr isotope ratios of ostrich egg shells from Nineveh in northern Iraq are slightly higher (0.708237(Q1)–0.708520 (Q3)) (Hodos et al., 2020). This slight discrepancy could arise from its location situated upstream of the confluence of the Tigris with eastern tributaries, or alternatively because some of the ostriches may have relied on mixed food/water sources partially related to the semi-deserts nearby (the ostriches were inferred to be wild rather than captive). Overall, the $^{87}Sr/^{86}Sr$ ratios for Zone 1 should be slightly over 0.708.

Sands in the Syrian semi-desert east of Raqqa display a very different ε_{Nd} of −12.3 (sidenote: $^{87}Sr/^{86}Sr$ = 0.709–0.710, nonbioavailable) (Henderson et al., 2020b). This ε_{Nd} value points toward a geologically older provenance, possibly related to siliciclastic materials derived from nearby uplifted formations of the Mesozoic and, to a lesser extent, Paleozoic ages, and/or aeolian deposition involving regional or remote dust sources. We expect similar scenarios for ε_{Nd} values in western Iraq, although no data have been reported from there. The arid areas in western Iraq and eastern Syria (Zone 2) have no bioavailable Sr isotope data reported. It is possible that the exchangeable Sr mainly originates from aeolian deposition as previously suggested for arid regions (Capo and Chadwick, 1999). On the other hand, Mesopotamia was once part of the Tethyan Seaway during the Miocene (Bialik et al., 2019). The strata of marine deposits should contribute low $^{87}Sr/^{86}Sr$ ratios (approximately 0.7085–0.7090 for seawater of the time, McArthur et al., 2012) to the labile Sr pool in eastern Syria or western Iraq (similar strata are beneath thick layers of Quaternary fluvial sediments in the Mesopotamian Plain, Yacoub, 2011). We thus tentatively suggest a combined effect of marine carbonate deposits and weathered silicate sediments for the regional bioavailable $^{87}Sr/^{86}Sr$ signature (analogous to Central Asian Zone 2), which should show a higher $^{87}Sr/^{86}Sr$ range than Mesopotamian Zone 1.

In eastern Syria, the sands of the Euphrates near Raqqa have ε_{Nd} values of approximately −2.1 (sidenote: $^{87}Sr/^{86}Sr$ around 0.708, nonbioavailable) (Henderson et al., 2020b), which is likely caused by the occurrence of mafic formations in the river's upper catchment in the mountains of southeastern Turkey. Soil from the archaeological site of Tell Leilan in the Khabur Plain in northeastern Syria yields an ε_{Nd} of −4.9 (Cullen et al., 2000). Plants from locations along the Euphrates and its branches in eastern Syria (including Raqqa) show $^{87}Sr/^{86}Sr$ of 0.70809(Q1)–0.70834(Q3) (Henderson et al., 2009).

Accordingly, due to sediment transport and fluvial deposition dominated by the Tigris, Zone 1 should feature relatively uniform isotopic signatures that are similar to those of the Zagros. The proposed ε_{Nd} range is from −4 to −6.5, while the regional bioavailable $^{87}Sr/^{86}Sr$ signature should fall around or slightly higher than 0.7080 but likely less than 0.7085. Hypothetically, northeastern Iraq may exhibit slightly lower ε_{Nd} values for detrital sediments (for instance, −8 to −6, using data from southern Iran as a reference). For Zone 2, aeolian deposition or erosion of old outcrops could have provided low-ε_{Nd} sand (for instance, <-8). Bioavailable Sr isotopic values for this zone can be assumed to be higher than 0.7085, but a better estimate is difficult due to a lack of data. In Zone 3, the Euphrates Valley before the river meets the deserts should largely retain isotopic signatures inherited from the river's upper course (for instance, $\varepsilon_{Nd} = -2$ to −5.5, $^{87}Sr/^{86}Sr$ approximately 0.7080–0.7085). The $^{87}Sr/^{86}Sr$ ranges proposed for Zone 1 and Zone 3 are relatively narrow, but we opt to keep these ranges for now to correspond with current data.

3.4. Short summary

We summarize the proposed isotopic zones and the estimated bioavailable Sr and detrital Nd isotopic ranges in Table 1 and illustrate them in Fig. 2.

Based on these ranges, we note that there are considerable overlaps between the different regions considered in this study, often reflecting similarities in geological and environmental settings among these regions (pure coincidences are possible; some are mentioned below). For example, a mix of mafic and felsic sources likely set the keynote for sediments derived from the Taurus-Zagros orogen, resulting in largely comparable Nd isotopic values in Mesopotamian Zones 1 and 3 and parts of Iran. Also, a repeatedly occurring mechanism is aeolian deposition, which needs to be considered for West and Central Asia but is still not well understood.

In many of the studied regions, geologic history and high evaporation (the latter is due to the arid/semi-arid climate) provide conditions for the buildup of calcareous contents in the surface horizons, profoundly affecting bioavailable Sr isotope ratios. In these areas, the common undertone is the shared 'geologic heritage' of once being part

of the Tethys or the Paratethys Sea. When these areas were cut off from the open ocean, shallow lagoonal conditions also widely occurred. In recent epochs, most of these regions have witnessed climate aridification and intensified aeolian dust events. Consequently, large parts are covered by sedimentary deposits composed of carbonate, evaporite, and siliciclastic layers. For instance, Cretaceous limestone and Jurassic shale are the most important parent rocks for soils in central and southern Iran, and are responsible for their high carbonate contents (Toomanian et al., 2001). In addition, the ubiquitous occurrence of gypsum in the arid soils of the Iranian central plateau can be traced to Lower Cretaceous marine evaporites (Khademi et al., 1997). These calcareous contents were typically originally introduced by colluvial fans and mountain runoffs, and their accumulation and distribution in soils are the result of dissolution and precipitation processes under arid/semi-arid conditions (Khademi et al., 1997; Khormali and Toomanian, 2018; Toomanian et al., 2001). Furthermore, a calcrete crust, which is developed by dissolution and precipitation of calcite under an arid/semi-arid climate, has been commonly observed in the surface facies of Euphrates deposits in Syria (Stow et al., 2020), although the origin of the calcium is not entirely clear (possibly aeolian dust). Based on the association of calcareous contents in the surface horizons with marine-derived calcareous sediments and aeolian deposits in these areas, we propose that their bioavailable Sr isotopic signatures likely reflect the Sr isotope ratio of past ambient seawater at the time of sediment deposition, supplemented by the effect of aeolian sorting and deposition which usually elevates the Sr isotope ratio.

The overlap between Mesopotamia (MP-1 and MP-3) and Iran in both Nd and Sr isotopic ranges potentially makes it difficult to discriminate between raw material sources in these areas. Also, the ε_{Nd} values for Central Asia outside the mountains (CA-2 and CA-3) may coincide with Iran and Mesopotamia, although they may mostly be differentiated using corresponding bioavailable Sr isotopic compositions. Similarly, the ε_{Nd} values for the Central Asian highlands (CA-1) and Iraqi/Syrian deserts (MP-2) also largely overlap, making bioavailable Sr isotopes particularly useful for separating them. On the other hand, thanks to contrasting ε_{Nd} signatures, it is possible to distinguish raw material sources in western Iraqi and eastern Syrian deserts (MP-2) from other Mesopotamian and Iranian sources. Siliciclastic materials from the Central Asian mountains (CA-1) also stand out from other Central Asian locations by their ε_{Nd} values.

We additionally note that isotopic signatures for peripheral regions may potentially overlap with the regions considered in this study. For instance, the Nd isotopic range for Levantine sands has been reported (Levantine coastal sands $\varepsilon_{Nd} = -7$ to -1, Henderson et al., 2020b; the Belus River mouth $\varepsilon_{Nd} = -4.8$ to -1, Brems et al., 2014), reflecting the Nile's sediment inputs into the eastern Mediterranean Sea. In Egypt, the Nile has a radiogenic sediment load characterized by an average $\varepsilon_{Nd} = -3.3$ (Goldstein et al., 1984; Weldeab et al., 2002) or ε_{Nd} values fluctuating between approximately -6 and -2 (Bastian et al., 2021), strongly influenced by fine materials from volcanic formations of the Ethiopian Highlands. Sands from the inland western deserts along the Nile in Egypt show $\varepsilon_{Nd} = -8.7$ to -6.0 (Brems et al., 2014), and sediments from Alexandria on the Mediterranean coast exhibit $\varepsilon_{Nd} = -8$ to -6 (Brems et al., 2013b). Meanwhile, Saharan dust is marked by its low ε_{Nd} value of approximately -13 (Grousset et al., 1998). The Indus Valley in Pakistan may be represented by the Indus River's sediments ($\varepsilon_{Nd} = -12.2$, Jeandel et al., 2007). The Nd isotopic signatures of these detrital sediment sources overlap with several zones in Mesopotamia, Iran, and Central Asia. In addition, human and faunal samples from inland Egyptian sites along the Nile exhibit a local average $^{87}Sr/^{86}Sr$ of 0.7077 (Buzon and Simonetti, 2013; Stantis et al., 2019). Samples from coastal locations may report $^{87}Sr/^{86}Sr$ ratios that are similar to that of seawater, thereby overriding any regional variation. For example, the southeastern tip of the Arabian Peninsula, including the northeastern UAE and northern Oman, exhibits $^{87}Sr/^{86}Sr$ ratios slightly lower than seawater (Gregoricka, 2013, 2014; Kutterer and Uerpmann, 2017). Coincidentally, materials from some locations in the continental hinterland (such as Central Asia Zone 2) also exhibit $^{87}Sr/^{86}Sr$ ratios in this range. Last, faunal samples from Bahrain (Gregoricka, 2013) display similar Sr ranges with Iran and, to a lesser extent, Iraq, which may be attributed to aeolian deposition by dust storms that sweep across the Middle East (see Section 4 in SM). Considering these potential overlaps, we need to keep geologically and archaeologically informed when interpreting similar Nd or Sr isotope ratios from different locations.

4. Provenancing plant-ash glass

Since ancient glass was often involved in long-distance trade, composition-based provenance is especially meaningful to reveal sociocultural links between the locations of production and usage (Lü et al., 2021). With the estimated isotopic ranges for the regions from Mesopotamia to Central Asia, we will now apply this Sr–Nd isotope baseline to plant-ash glass provenance. Our goal is twofold: first, since our baseline has been constructed entirely from environmental and bioarchaeological information without using any glass data, we will verify whether this baseline contributes to an understanding that is consistent with established provenances of archaeological glass. Second, we will see if our integrative Sr–Nd isotope approach can bring a new understanding of archaeological glass provenance (i.e., ascertaining or narrowing down possible origins). We will show that the Sr–Nd isotope baseline indeed provides essential geochemical guidance, with which the proposed origin of glass artifacts or raw materials can be verified.

In plant-ash glass, Sr is mostly brought in with the lime content in plants (minor contributions from minerals such as calcite, feldspar, and pyroxene in the silica raw material are possible), reflecting the bioavailable Sr of the environment where the plants grew (Degryse et al., 2010c; Freestone et al., 2003). Nd in plant-ash glass mostly originates from the non-quartz minerals in silica material (Brems et al., 2013b), such as detrital clay minerals. The Nd levels in halophytic plants are negligible (Barkoudah and Henderson, 2006). The potential contribution of Nd contents from clay adhering to the plants or contamination from the crucible or grinding tools is minor (Degryse et al., 2015), and such contamination was also unlikely to happen for any large-scale manufacture of glass. Therefore, the Sr and Nd isotope ratios serve as unique indicators for the origins of flux and silica raw materials respectively, allowing for independent provenance for the two main ingredients.

To properly provenance glass artifacts, both chemical and isotopic compositions need to be considered. Isotopic information alone is not a one-size-fits-all tool. For example, as mentioned above, the ε_{Nd} range of Levantine coastal sand largely coincides with that of Mesopotamia detrital sediments. However, for plant-ash glass provenance, the chemical composition of Levantine glass is typically distinct from Mesopotamian glass (e.g., distinguished by the MgO/CaO ratio, Henderson et al., 2016). In echoing previous researchers who advocated a multi-proxy approach in mobility studies (e.g., Holt et al., 2021; Knudson and Price, 2007; Wu and Zhang, 2022), we stress that a combination of chemical and multiple isotopic compositions is more likely to reduce the ambiguity in glass origins that are often observed with one type of tracer alone.

The availability of Sr and Nd isotope data also opens fresh opportunities to investigate glass 'recycling'. Isotope mixing models have been used in archaeology, for example, with Sr isotopes for mobility studies (e.g., Bentley, 2006; Lengfelder et al., 2019; Montgomery et al., 2007), Sr, Pb, and Nd isotopes for glass (Degryse et al., 2006; Henderson et al., 2015), Sr isotopes for ceramics (Henderson et al., 2020a), and Pb isotopes for metallurgy (Pernicka, 2013; Pollard and Bray, 2015). Here, using two-endmember mixing lines of ε_{Nd} vs 1/Nd, we examine potential glass recycling practices associated with medieval plant-ash glass from the Silk Road regions. This is a more appropriate way than the ε_{Nd} vs Nd plot to present Nd isotope data because mixing relationships between two separate endmembers generate linear trends in the ε_{Nd} vs 1/Nd

graph. The geochemical context provided by the isotope baseline can also be very indicative of the mixing endmembers. We suggest that an integrative approach, based on the complementary use of the Sr–Nd isotope baseline and isotope endmember mixing plots, in addition to the widely used chemical and isotopic composition clustering, offers the most consistent provenance results.

We also underscore the unique bioavailable $^{87}Sr/^{86}Sr$ signatures (>0.7095) for Central Asia Zone 1 and Zone 3. Almost no isotopic investigation of Central Asian excavated glass has been reported, except for the brief mention of 'Central Asian chemical type' glass from Xinjiang, China, which bears $^{87}Sr/^{86}Sr$ ratios of 0.710–0.716 (Brill and Fullagar, 2009). This range falls into our proposed Central Asian Zones 1 and 3, suggesting that the plant ash used to make these glasses or the glass products themselves may have originated from the mountainous or piedmont loess areas in eastern Central Asia. This is consistent with existence of historical population centers (such as the Fergana Valley) in eastern Central Asia and the close contact of this area with Xinjiang. We emphasize that our proposed $^{87}Sr/^{86}Sr$ range was obtained by using qualitative reasoning and data from environmental proxies. Therefore, this match with glass data also confirms the validity of our baseline construction method.

4.1. Case study 1: plant-ash glass from Mesopotamia

In this study, we apply our integrative Sr–Nd isotope approach to investigate the provenance of Mesopotamian plant-ash glass. Islamic plant-ash glass from the Levant has been included for comparison. The compared datasets include plant-ash glass from Raqqa, Syria (Islamic) (Henderson et al., 2009), Veh Ardashir, Iraq (Sasanian) (Ganio et al., 2013), Dibba, UAE (1st C. CE) (Van Ham-Meert et al., 2019), Tell Brak, northeastern Syria, Nuzi, northeastern Iraq, and Nippur, southern Iraq (LBA) (Degryse et al., 2010a, 2015; Henderson et al., 2010), Damascus, Beirut, and Serçe Limani (Islamic) (Brill, 1999; Henderson et al., 2020b), and Tyre and Banias (Islamic) (Degryse et al., 2010b). Here, we have distinguished between raw glass (raw furnace glass or glass ingots/chunks), which indicates the occurrence of glass production, and manufactured glass objects. Fig. 3 displays the comparison of $^{87}Sr/^{86}Sr$ ratios for biological and glass samples. The ε_{Nd} comparison, as well as the relationships given by Sr–Nd isotopes, is illustrated in Fig. 4.

In Fig. 3, almost all samples show $^{87}Sr/^{86}Sr$ ratios below modern seawater. A relative homogeneity of $^{87}Sr/^{86}Sr$ is observed: $^{87}Sr/^{86}Sr$ ratios in Fig. 3 are actually within a relatively small interval for a variety of samples from a vast area, especially when compared to bioavailable $^{87}Sr/^{86}Sr$ ranges in many other regions that are known to display a much greater $^{87}Sr/^{86}Sr$ variability (for example, China, Wang and Tang, 2020). As discussed above, this relative uniformity of $^{86}Sr/^{87}Sr$ compositions most likely reflects the fact that bioavailable Sr signatures in these regions are controlled by weathering of marine-derived sedimentary rocks. For Mesopotamia and Iran, we calculated the bioavailable Sr isotopic range (average ± 2 s.d. = 0.707728–0.708631, blue lines in Fig. 3) from excavated faunal and human samples (western deserts are likely outside this range). Note that 2 s.d. are inherently relatively conservative (i.e., broad) for the actual local ranges. In Fig. 3, almost all Mesopotamian glass samples, including most raw glasses from Raqqa, Veh Ardashir, and Tell Brak, and most vessels from Raqqa, Nuzi, and Veh Ardashir, fall into this Mesopotamian-Iranian isotopic range indicated by the blue lines. This range corresponds to the isotopic zones of MP-1, MP-3, and Iran, suggesting that the majority of Mesopotamian glass was probably made using plant ash from Mesopotamia (except for MP Zone 2) or Iran, and that Mesopotamian deserts/semi-deserts (Zone 2) were likely not among the main origins for the ashed plants. Compared to Iran, Mesopotamia is more likely the origin of the plant ash with more excavated glass reported from there, but glass-making using Iranian plants may not be distinguished on the basis of Sr isotopes. Not all halophytic plant species are suitable for fluxing in glass-making. The fact that large quantities of glass objects demonstrate similar $^{87}Sr/^{86}Sr$ ratios may indicate either common sources of plant ash or similar geology/ecology from which the plants derived. The first possibility implies one or more supply centers of plant ash, while the second possibility suggests a likely consistent practice of ashing similar species of plants harvested from similar environments.

Although our proposed bioavailable Sr isotopic ranges for MP-1 and MP-3 overlap, there are still minor but discernible differences in Sr isotopic distribution patterns: based on reported biological samples from MP-1 (Ur and Mashkan Shapir in southern Iraq, and Bestansur in northeastern Iraq, but excluding Nineveh ostrich egg shells) and from MP-3 (plants from locations in the Euphrates Valley in Syria), most of MP-1 likely has a lower average bioavailable $^{87}Sr/^{86}Sr$ than MP-3. In Fig. 3, almost no glass corresponds isotopically to the southern Iraqi (or Bestansur) biological samples (below the gray dashed-line box in Fig. 3), implying that the plants used for glass-making likely did not come from the floodplain (MP-1 regions). The Sr isotopic composition of most LBA glasses (Tell Brak, Nippur, Nuzi) seems to better align with that of the Euphrates Valley or Nineveh biological samples (inside the gray box in Fig. 3), which suggests that river valleys in northern Mesopotamia could be the main source of plant ash for LBA glass-making. Interestingly, even glass discovered in Nippur, located in southern Iraq, does not quite align with southern Iraqi faunal/human samples in $^{87}Sr/^{86}Sr$ ratios, meaning

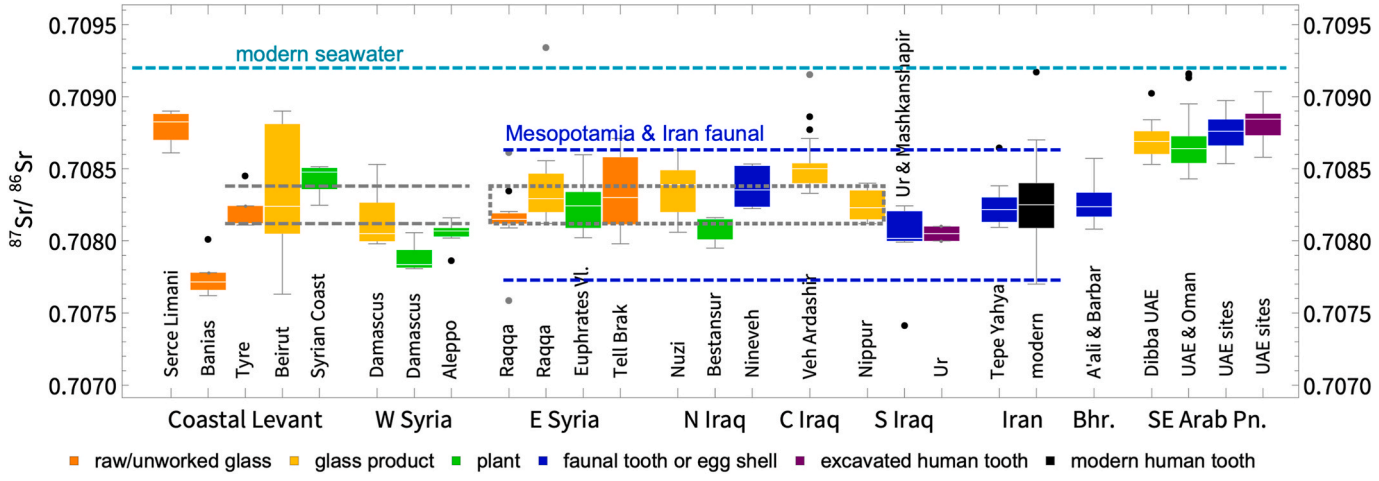

Fig. 3. (Color online) Sr isotopic composition of glass, plant, faunal and human samples in West Asia. The range of Mesopotamian and Iran faunal samples (average ± 2 s.d., blue dashed line) and the most concentrated isotopic range of the glasses (gray box and gray line) are indicated. Refer to Table S1 (Section 1 in SM) and the text for data sources.

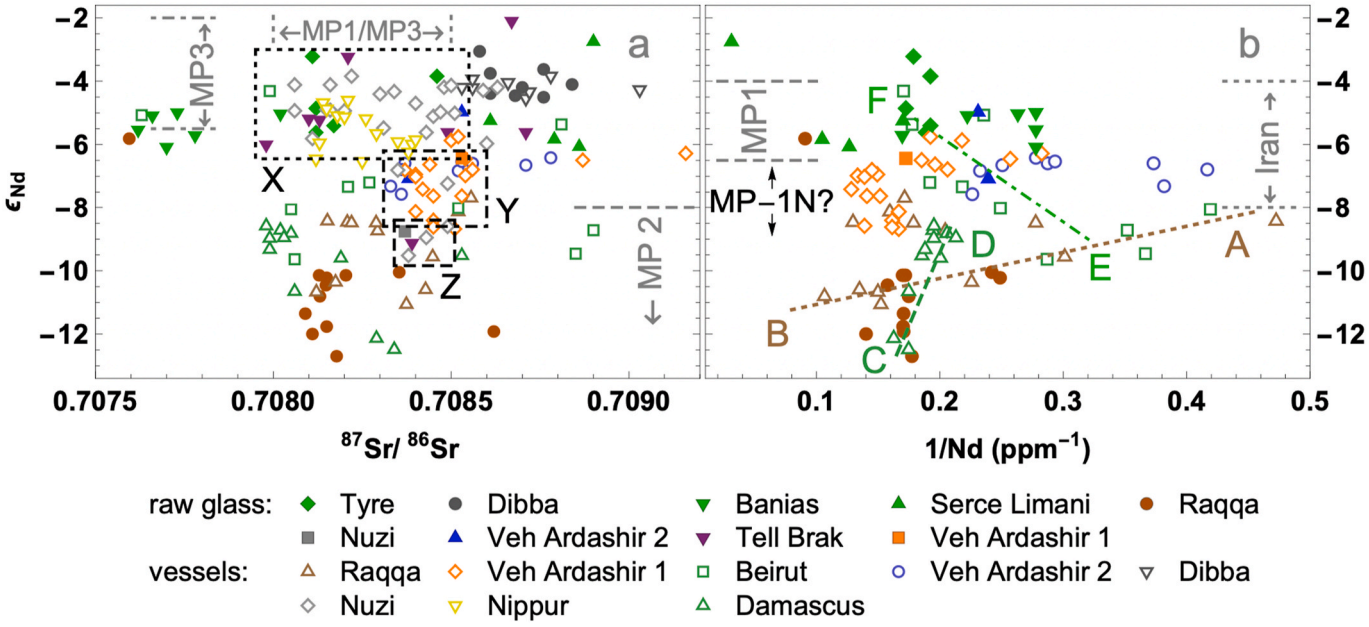

Fig. 4. (Color online) Nd–Sr isotopes for raw glass and glass vessels: (a) relationship between ε_{Nd} and $^{87}Sr/^{86}Sr$ and (b) ε_{Nd} vs 1/Nd. Dotted box X: most of LBA glass; dot-dashed box Y: most Sasanian glass from Veh Ardashir; dashed box Z: a small group of LBA glass; brown dotted line AB, green dashed line CD, green dot-dashed line EF: mixing lines indicating remelting practices for Raqqa, Damascus, and Beirut vessels, respectively. Vessels are indicated by open symbols while raw glass is indicated by solid symbols. Refer to Table S2 (Section 1 in SM) and the text for data sources. Not all samples have Nd concentrations reported.

that glass from Nippur was possibly also made using plant ash from northern Mesopotamia. The use of this northern source of plant ash may have continued or revived later, since Islamic glass vessels from Raqqa show similar Sr isotopic signatures.

Additionally, we observe that the $^{87}Sr/^{86}Sr$ ratios for Veh Ardashir samples (and some Nuzi, Tell Brak, and Raqqa samples) are above the data plotted in the gray box in Fig. 3. It is possible that a different source of plants was used for making these glasses during the LBA, the Sasanian period, and the Islamic period. The $^{87}Sr/^{86}Sr$ ratios typically exhibited by these samples are near the upper end of the MP-1/MP-3 ranges, but are not radiogenic enough to be attributed to MP-2. Meanwhile, Veh Ardashir samples are comparable in $^{87}Sr/^{86}Sr$ to the upper half of the range given by Nineveh ostrich egg shells, implying a possible link. Also, several Veh Ardashir objects exhibit even higher $^{87}Sr/^{86}Sr$ ratios deviating toward 0.709. Geographically, Veh Ardashir is adjacent to Ctesiphon south of today's Bagdad, and its local Sr isotopic signature should align mostly with the $^{87}Sr/^{86}Sr$ range of Mesopotamian Floodplain, but this is apparently not the case reflected in Veh Ardashir glass. This hints that the plants used for glass-making could have grown in areas with slightly more radiogenic $^{87}Sr/^{86}Sr$ signatures in northern Mesopotamia, for example, semi-arid environments near the river valleys where aeolian-sourced strontium probably has a minor contribution, and the area near Nineveh is a possible candidate. Also, the similar $^{87}Sr/^{86}Sr$ ratios in some of the glass artifacts from Tell Brak and Raqqa indicate that this plant ash source was possibly also accessible for the Euphrates Valley settlements in Syria. Considering that both Nineveh and Veh Ardashir are located on the Tigris, one possibility is that the movement of materials or products was facilitated by the river. If, however, plant ash was from areas near the Euphrates Valley in northern Mesopotamia, transportation of goods via the Euphrates would also be viable. The 9th-century Islamic capital, Samarra, where compositional evidence is considered supportive of glass production (Henderson et al., 2016; Schibille et al., 2018), is to the north of Baghdad on the Tigris. Future Sr isotopic analyses on Islamic glass from Samarra and Ctesiphon could help delineate the temporal and geographical extent of the use of this type of plant ash.

Levantine glasses vary widely in $^{87}Sr/^{86}Sr$ ratios. As already noted in previous research, both coastal and inland plants had been exploited for Levantine glass-making (Degryse et al., 2010b; Henderson et al., 2020b). The broadly variable Nd–Sr isotopic signatures of Beirut and Damascus vessels (Figs. 3 and 4(a)) show that the metropolitan centers likely attracted glass merchandise from different regions. Significantly, in Fig. 3, a considerable portion of the Beirut, Damascus, and Tyre glasses do not align with coastal Levantine or western Syrian plants but fall into the Mesopotamian-Iranian range. Mesopotamia might have provided plant ash or glass products for the Levant (Iran is less likely due to its distance from the Levant). We will return to this later with a discussion based on further evidence from Nd isotopes. Nonetheless, it has been reported that the $^{87}Sr/^{86}Sr$ ratios of plants and invertebrates in northern Israel vary from 0.7074 to 0.7090, mainly resulting from the Tethys sedimentary deposit and varied lithologies (Hartman and Richards, 2014), which overlaps with the range for Mesopotamia. Hence, the possibility of using ashed plants mostly from near the Levant cannot be excluded.

Concerning Nd isotopes, LBA glass vessels from Nuzi and Nippur and raw glass from Tell Brak (dotted-line box X in Fig. 4(a)) mostly fall into the ε_{Nd} ranges of MP-1 and MP-3. With the overlapping isotopic ranges, we are unable to ascertain the exact sources of silica based on current evidence. However, considering the generally low impurity levels of LBA Mesopotamian glass (e.g., Tell Brak glass Nd ~ 1 ppm, Henderson et al., 2010; Nuzi glass $Al_2O_3 < 1\%$, $Fe_2O_3 < 0.5\%$, Degryse et al., 2010a; Nippur glass $Al_2O_3 < 1.5\%$, Fe ~ 5000 ppm, Cr $\lesssim$ 30 ppm, Walton et al., 2012), silica materials (e.g., quartz pebbles) from northern Mesopotamia were more likely to have been involved than silt-rich sands from the fluvial deposits in southern Mesopotamia.

Notably, most Sasanian raw glass and glass vessels from Veh Ardashir fall into the intermediate ε_{Nd} range of −8.5 to −6.0 (dot-dashed-line box Y in Fig. 4(a)). The ε_{Nd} values of these artifacts agree with the range for Iran or MP-1N — an extended range of MP Zone 1 potentially existing in northeastern Iraq and showing slightly lower ε_{Nd} signatures. Data for Veh Ardashir raw glass are within the ε_{Nd} ranges of MP-1 and the putative MP-1N, likely indicating that Sasanian glass production indeed exploited silica sources related to the Zagros geology. Previously, it has been pointed out that different silica materials were used for

different groups of Veh Ardarshir glasses (Mirti et al., 2009). It is possible that the silica materials used to make Veh Ardashir glasses (and other glasses related to MP-1N) were from the same general geological background (thus having similar ε_{Nd} values) but with different weathering or erosion conditions.

A small amount of LBA Mesopotamian glass, mostly from Nuzi, shows ε_{Nd} values between −10 and −8.5 (dashed-line box Z in Fig. 4(a)), consistent with the range for MP Zone 2. These artifacts include one glass ingot from Tell Brak and one ingot from Nuzi, implying that this type of silica or raw glass was likely within their reach. This suggests that desert/semi-desert sands in northern/western Iraq and eastern Syria were probably exploited for glass-making as early as the Bronze Age. During the Islamic period, Raqqa raw glass, possibly made using Syrian semi-desert sand, has ε_{Nd} values lower than −10 (Henderson et al., 2020b). The continued or revived use of this type of silica material also concurs with the use of northern plant ash suggested above, showing that Raqqa's Islamic glass-making industry probably employed similar local raw materials to those used during the LBA.

Curiously, in Fig. 4(a), vessels from Beirut, Damascus, and Raqqa are not close to Levantine and Raqqa raw glasses in Sr and Nd isotopic compositions, and were suggested to be products from either a different type of primary glass or mixed glass (Henderson et al. 2020b). Here, we suggest that this disparity in isotope ratios is due to glass mixing/-recycling, in which the isotopic signature of imported glass was gradually taken over by locally made glass that was added with each remelting (the original chemical compositions were also diluted in this process). We demonstrate this in Fig. 4(b) with ε_{Nd} vs 1/Nd relations, in which the distribution of data points on such 'binary mixing lines' are suggestive of glass recycling practices and displays the endmembers that were mixed in.

For Raqqa vessels (brown dotted line AB), the mixing of glasses likely occurred, starting with glass at Point A (9th century vessel), which is characterized by $\varepsilon_{Nd} \sim -8.5$ and a very low Nd concentration (~2 ppm), and going on a trend toward ε_{Nd} values and Nd levels that are typical of Raqqa raw glass (Point B, 9th–12th century vessels). This shows a recycling process in which imported high-quality glass made using low-impurity silica materials, possibly crushed quartz pebbles from MP-1N, was gradually diluted by repeated addition of glass vessels (or less likely, raw glass) that were made using local sands from MP-2 semi-deserts. The occurrence of glass mixing was previously suggested for some of Raqqa glass (Henderson et al., 2004). The glass with an extremely low Nd level and a possible Iraqi origin, represented by Point A, is reminiscent of the high-quality Islamic glass from Samarra (Henderson et al., 2016; Schibille et al., 2018), a potential link that is worth further investigation.

For Damascus vessels (green dashed line CD), a similar process likely took place, starting with Raqqa-type glass with very low ε_{Nd} values (Point C, 12th century vessels). Glass characterized by $\varepsilon_{Nd} \sim -9$ and Nd concentrations ~ 5 ppm, possibly locally made, was then added through repeated remelting (Point D, 12th–14th century vessels). Since western Syria to the east of the Anti-Lebanon Range was marked by deserts and the Palmyride fold belt, which are largely comparable to MP-2's conditions for detrital sediments, it is possible that silica sources from large parts of western Syria exhibit ε_{Nd} signatures similar to MP-2 (although their bioavailable $^{87}Sr/^{86}Sr$ ratios could be considerably different, as shown by plant samples from western Syria in Fig. 3). For Point D, although silica materials (or glass products) from northern Iraq (MP-1N) also possess comparable ε_{Nd} levels, the constant use of imported glass or raw materials from distant locations for remelting when glass from nearer locations was available seems unlikely.

In addition, Beirut vessels may have also undergone recycling processes, starting from imported Mesopotamian glass and replenished by local Levantine glass (green dot-dashed line EF). The compositional signatures of Beirut vessels are more variable on the Mesopotamian end (Point E), shown as a string of scattered points on the Raqqa mixing line AB. A possible explanation is that Raqqa's reworked glass products containing varying portions of northern Iraqi glass were possibly brought to Beirut, which were subsequently reused by adding Levantine glass. Most of the Beirut data are from the 12th–14th century vessels.

If the above deductions about glass mixing hold, we may further suggest a westward diffusion pattern of Islamic plant-ash glass from Mesopotamia to Syria-Palestine during the period of the 9th–14th century. In this diffusion, glasses from Mesopotamia were recycled in a melt of locally made glass at major Middle Eastern metropolises in the trade network.

Glass recycling was likely widespread and common in history but is still difficult to ascertain in provenance research (Rehren and Freestone, 2015), and its occurrence during the Islamic period was also affirmed by the cullet carried by the 11th-century Serçe Limani shipwreck (Bass et al., 2009). Benefiting from isotopic ranges for different zones and the use of Nd isotope mixing lines, we have provided compositional evidence for the recycling practice of Islamic plant-ash glass. It was likely that, simultaneously with primary glass production in the Islamic world, recycling of broken glass widely occurred, involving glass products that reached the end of their use life. It is almost certain that recycling was not limited to the above scenario in which imported glass was mixed into locally made glass. Glass products made entirely from recycled local glass should have been common. However, remelted glasses from different production zones allow us to identify the occurrence of glass recycling precisely because only in such cases can a mixing line be drawn between drastically different chemical/isotopic signatures.

The above analysis of plant-ash glass recycling also implies that part of the glasses traded were probably remade products from an intermediate location on the trade route while the chemical and/or isotopic signatures of the original primary glasses were 'masked'. This confirms that the dispersion and recycling of glass may have been intertwined processes. This has ramifications on composition-based provenance studies and prompts us to suggest that an examination of ε_{Nd} vs 1/Nd relations should be included in isotopic provenance studies when possible.

To summarize, using our integrative Sr–Nd isotope approach, we have suggested that northern Mesopotamia may have been a supply center for glass-making raw materials over a long period, likely having provided at least two types of plant ash from different environments near river valleys (MP-3 or MP-1) and two types of silica materials related to mountain-derived clastic rocks and desert sands (MP-1N and MP-2). Using Nd isotope mixing line, we have also revealed the practice of glass recycling for Islamic plant-ash glass.

4.2. Case study 2: provenance of San Lorenzo glass

In this study, we assess the provenance of the medieval plant-ash glass from San Lorenzo, Apulia, Italy, dated to the 12th-14th century. Sr and Nd isotopic compositions were reported for 12 samples (Gliozzo et al., 2021). The 12 samples from San Lorenzo include SLC3 (goblet), SLC7 (from prunted beaker group 1), SLC9–10 (from prunted beaker group 3), SLC12 (beaker), SLC13–14 (bottles), SLC21–24 (lamps), and SLC25 (vessel base). Based on a comparison with European and Middle Eastern plant-ash glasses, Gliozzo et al. inferred possible Mediterranean or Mesopotamian origins for the San Lorenzo artifacts, where a Mediterranean provenance was used to broadly indicate Levantine, Syrian, or Adriatic origins, while a Mesopotamian provenance mostly referred to central Iraq. Our use of these geographic terms is somewhat different. Most notably, we use 'the Eastern Mediterranean' to refer to the coastal strips only (mainly Egypt and the Levant) and consider Raqqa as an inland site in northern Mesopotamia. For SLC3, SLC9, SLC10, and SLC21, Gliozzo et al. also suggested partial similarities with certain Italian samples. Three samples, SLC14, SCL22, and SLC23, were without a match and no provenances were suggested.

In Fig. 5, we compare the Sr and Nd isotopic compositions of San Lorenzo glass with Levantine and Mesopotamian Islamic/Sasanian plant-ash glasses (Degryse et al., 2010b; Ganio et al., 2013; Henderson et al., 2009, 2020b), and compare their chemical compositions with

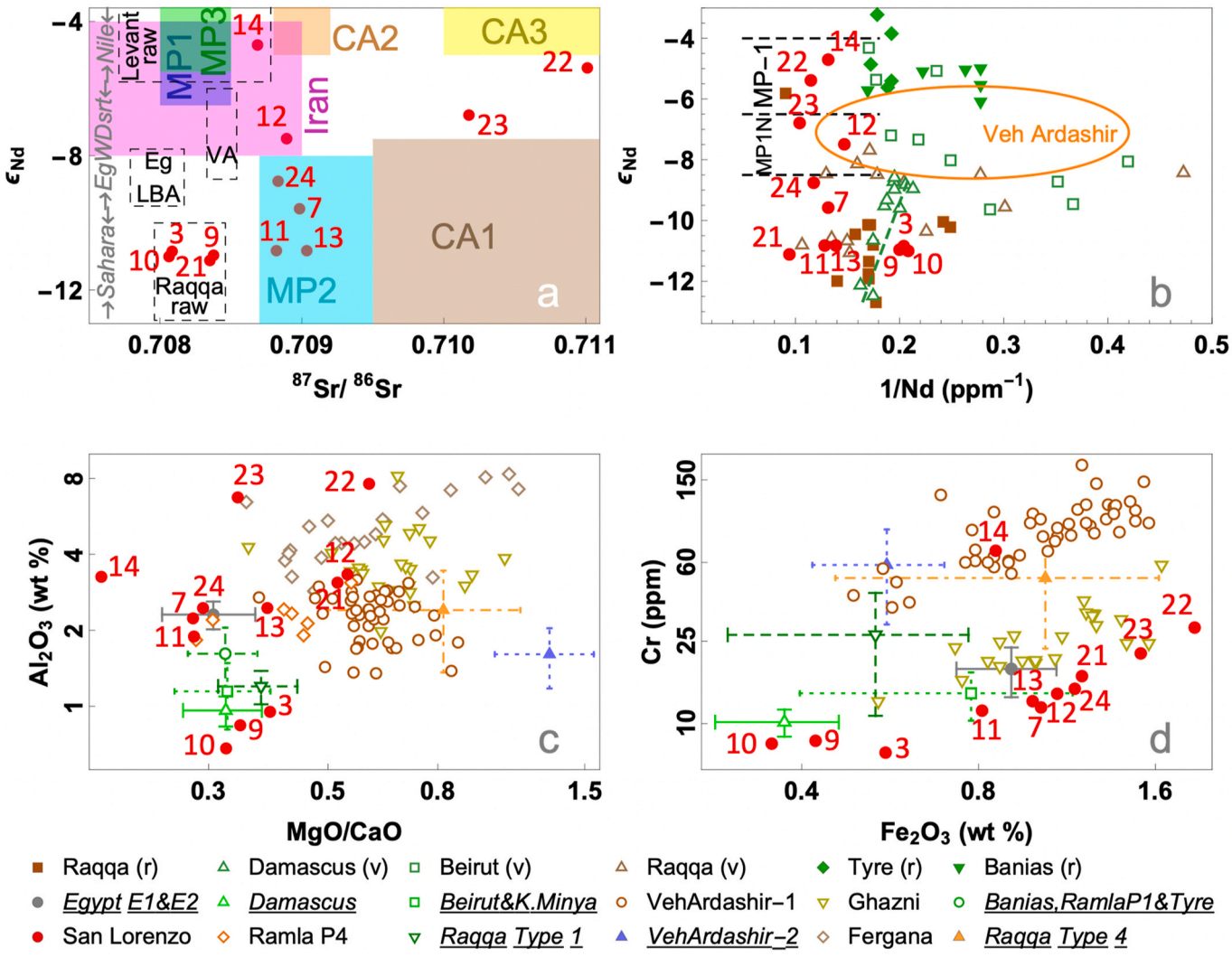

Fig. 5. (Color online) (a) Nd–Sr isotope ratios for San Lorenzo glass in the context of the isotopic zones. (b) ε_{Nd} vs 1/Nd. (c) Al_2O_3 vs MgO/CaO. (d) Cr vs Fe_2O_3. San Lorenzo samples are marked by red-colored sample numbers. Refer to the text for data sources for these plant-ash glasses. Some of the datasets are represented by average values and standard deviations (*underlined and italicized* in the legend) so that the graph is not overcrowded. (r) and (v) in the legend indicate raw glass and vessels, respectively.

Islamic plant-ash glasses from Egypt (Groups E1 and E2) (Schibille et al., 2019), the Levant (Beirut and Khirbat al-Minya, Henderson et al., 2016; Damascus, Henderson et al., 2016; Ramla, Phelps, 2018; Tyre, Freestone, 2002; Banias, Freestone et al., 2000), Mesopotamia (Raqqa, Henderson et al., 2004, 2016), and Central Asia (Ghazni, Fiorentino et al., 2019; Akhsiket and Kuva in Fergana, Rehren et al., 2010), as well as Sasanian glass from Veh Ardashir in Mesopotamia (Mirti et al., 2008, 2009).

With uniquely high $^{87}Sr/^{86}Sr$ ratios, SLC22 sits close to CA-3 in Fig. 5 (a), suggesting it was possibly made in the piedmont loess area (the use of sands from CA-2 and plant ash from CA-3 is also a possibility), while SLC23 appears closer to CA-1, i.e., the mountainous area. The chemical compositions of these samples also fall into Central Asian glasses, which are rich in Al and Fe, as shown in Fig. 5(c)(d). With high Nd concentrations, SLC22 and SLC23 lie in the upper left corner in Fig. 5(b). SLC14's ε_{Nd} value is in the range of the Levant or Mesopotamia, and its $^{87}Sr/^{86}Sr$ ratio is similar to Levantine raw glass but still close to the Mesopotamian ranges (Fig. 5(a)). Its Al, Cr, and Fe levels, typically considered related to the silica source, are consistent with Mesopotamian glass, but its MgO/CaO is distinctly low, a signature for Levantine glass (Fig. 5(c)(d)). Thus, SLC14 can be identified as Mesopotamian glass but with possible Levantine influence. SLC21's Sr and Nd isotopic compositions imply a Mesopotamian (especially Raqqa) origin (made using MP-2 sands and MP-1/MP-3 plant ash), and its chemical composition in Fig. 5(c)(d) is also close to Mesopotamian glass (although almost on the edge with Central Asian glass, possibly due to variation in impurities in Mesopotamian desert sands).

SLC3, SLC9, and SLC10 are in the same isotopic range as Raqqa raw glass in Fig. 5(a), whereas in Fig. 5(c)(d), they align with Levantine glasses and are closest to Damascus vessels. We have discussed above that the analyzed Damascus vessels were probably made from mixing Raqqa glass with locally made glass. SLC3, SLC9, and SLC10 could have been produced from a similar process, as they are also on the mixing line (colored green) in Fig. 5(b). In Gliozzo et al. SLC12 was inferred to have a Mesopotamian origin since its ε_{Nd} value matches that of Veh Ardashir glass. In fact, SLC12's isotopic signatures in Fig. 5(a) can lead to different explanations. We note that its Al, Cr, and Fe concentrations are often in line with Central Asian glasses. In Fig. 5(b), SLC12 can be considered to be on a hypothetical mixing line connecting Central Asian glasses (SLC22–23) with Mesopotamian glass (e.g., Veh Ardashir glass). Therefore, SLC12 may possibly have been produced by mixing Central Asian and Mesopotamian glasses. Another explanation, considering the possibility of plant ash trade, is that SLC12 was made using silica materials from CA-1 and plant ash from Iran or CA-2.

For SLC7, SLC11, SLC13, and SLC24, a probable connection with Raqqa glass was suggested based on Nd isotope ratios. From Fig. 5(c)(d), we note that their Al, Cr, and Fe concentrations are not consistent with Raqqa Type 1 or Type 4, but most closely align with Egyptian glass. In Fig. 5(a), their ε_{Nd} values agree with the ranges for Egyptian inland western desert and the Sahara Desert (Brems et al., 2014; Grousset et al., 1998), and their $^{87}Sr/^{86}Sr$ ratios can be explained by a potential plant ash source under the influence of sea spray or similar to the plant ash used to make Serçe Limani glass (also within the nonbioavailable $^{87}Sr/^{86}Sr$ range for Egyptian desert sands, Brems et al., 2014). If these artifacts were indeed produced in Egypt, their isotopic signatures are separated from LBA Egyptian plant-ash glass ($^{87}Sr/^{86}Sr$ = 0.70780–0.70817, Brill and Fullagar, 2009; Degryse et al., 2015; Henderson et al., 2010; and ε_{Nd} = −7.8 to −9.5, Degryse et al., 2015; Henderson et al., 2010), indicating that different glass-making materials were used.

The identification of Central Asian glass in San Lorenzo is noteworthy. It was perhaps not uncommon for Central Asian glass to have arrived in medieval Europe despite the geographical separation. A wheel-cut bowl in Venice with an assigned date of approximately 1000 AD has an inscription of 'Khurasan' on the bottom (Kröger, 1995), indicating its likely origin from the Khorasan region between Iran and Central Asia. Here we have also indicated that some of the San Lorenzo glass was probably made from a mix of remelted glasses from different origins, again suggesting that glass recycling at the time was likely common. It was likely that many Central Asian and Mesopotamian glass pieces underwent recycling processes and were transformed into Eastern Mediterranean products before they reached Europe. Perhaps, part of the glasses received by Italy from the Eastern Mediterranean were reworked glass products, which were then remelted again to manufacture objects that exhibit Italian, French, and other European designs such as those found in San Lorenzo.

Using the integrative isotope approach, our analysis has reached similar conclusions for some of the San Lorenzo glasses to those proposed in Gliozzo et al. However, we have suggested alternative possibilities for others in the assemblage. More reported data will help ascertain their exact origins. It should still be noted that Italy has a history of primary glass production. However, since very different compositions have been identified in San Lorenzo glass vessels of similar styles, this compositional diversity implies that primary raw glass was probably not constantly available for the workshops in the region. In the above analysis, our isotope baseline provides an essential geochemical context for comparing isotopic compositions and has been a useful guide when chemical information is incomplete or ambiguous. In particular, with a lack of isotope data for glass from Central Asia, the baseline fills a crucial gap and proves to be helpful.

5. Conclusion

We have established the first semi-quantitative bioavailable Sr and detrital Nd isotope baseline for the Silk Road regions of Central Asia, Iran, and Mesopotamia. Three isotopic zones for Central Asia and three isotopic zones for Mesopotamia have been proposed, although only one general range for Iran has been proposed due to limited data. The isotopic signatures of these zones are controlled by geologic history, environmental conditions, and Earth surface processes. To varying extents, Mesozoic-Cenozoic marine and continental sedimentary deposits predominantly set the isotope geochemical background for most of these zones. Our exploration showcases the potential of utilizing reported data from Earth and environmental sciences for the benefit of archaeological research. Except for plant-ash glass, the regional isotope baseline may also be used for other archaeological materials such as ceramics.

Aided by this isotope baseline as an indispensable geochemical guide and applying isotope mixing lines, we have suggested that glass recycling occurred in Islamic plant-ash glass. We have inferred northern Mesopotamian origins for the raw materials used to make Mesopotamian glass, and suggested diverse provenances in Mesopotamia and Central Asia for glasses found at San Lorenzo. Our analysis also indicates that Nd isotopes may have great potential as a useful tool in plant-ash glass provenance, especially if more reference data become available in the future.

Admittedly, the available dataset is still sparse for such a vast and geochemically varied region, and we have only treated spatial variability on a very coarse level. For Central Asian basins and the Mesopotamian Floodplain, where lithology and environmental conditions are relatively homogeneous, sparse data coverage may be acceptable. However, for geologically complex areas such as the Central Asian mountains and Iran, currently available data may not sufficiently reflect the spatial variability of isotopic compositions. For certain areas such as western Iraq, northeastern Iraq, and Central Asian loess, due to the lack of data, the results have been mostly obtained by drawing parallels with nearby areas and by qualitative investigations. More data and a better understanding of surface conditions are needed to improve the quality of the baseline. In this regard, we note that this work should be viewed in the context of generating useful information with limited available data, a scenario often encountered in archaeology. We consider our estimate of isotopic signatures as a crude sketch to demonstrate only the macroscopic isotopic patterns, or as a zeroth-order approximation awaiting higher-order corrections. We anticipate our baseline as a starting point that will be refined by future regional studies on specific materials that are archaeologically more relevant.

The impact of climate and environmental change may significantly alter the regional isotopic signature. One such example is the Nile. Sediment cores show that the change in rainfall caused the contributions from major sediment sources to fluctuate significantly, leading to marked changes in Sr and Nd isotope ratios in the Nile floodplain and delta over the Holocene (Bastian et al., 2021; Stanley et al., 2003; Woodward et al., 2015). This underscores the future need to incorporate paleoenvironmental studies and take temporal shifts in isotopic patterns into consideration. Furthermore, we have not considered sampling depths for the data. It has been known that roots taking up Sr at different depths affect the $^{87}Sr/^{86}Sr$ ratio of plants (Poszwa et al., 2004), and Nd isotopic compositions may also differ for soils at different depths (Aubert et al., 2001). Although not practical for 'retrospective' data aggregation, a consideration of vertical profiles should be included for future 'prospective' sampling.

CRediT author statement

Qin-Qin Lü: Conceptualization; Data curation; Formal analysis; Funding acquisition; Investigation; Methodology; Project administration; Resources; Validation; Visualization; Writing - original draft; Writing - review & editing. Yi-Xiang Chen: Formal analysis; Methodology; Validation; Writing - review & editing. Julian Henderson: Methodology; Validation; Writing - review & editing. Germain Bayon: Methodology; Validation; Writing - review & editing.

Declaration of competing interest

The authors declare that they have no known competing financial interests or personal relationships that could have appeared to influence the work reported in this paper.

Acknowledgements

The authors would like to thank Prof. Zihua Tang (Institute of Geology and Geophysics, CAS) for constructive comments and Prof. Ruizhi Yang (USTC) for important facility support. The authors appreciate helpful suggestions from Prof. Changsui Wang (UCAS), Prof. Liqun Dai (USTC), Prof. Xingxiang Zhang (USTC), Dr. Xiaotong Wu (USTC), and David Redhouse (University of Cambridge). The authors gratefully acknowledge support from the University of Cambridge. Q.-Q. Lü would

like dedicate this work to Dr. Hai-Wei Long (1984–2015) of Shunde, Guangdong, a promising high energy physicist, an art and music lover, a guardian for the underprivileged, a true friend, and a noble soul. Dr. Long will be sorely missed.

This research was supported by the National Natural Science Foundation of China (Grant No. 12005222) and USTC Research Funds of the Double First-Class Initiative (Key Innovation Project for Early Career Investigators No. YD2110002005), both awarded to Dr. Lü.

Appendix A. Supplementary material

Supplementary material to this article can be found online at https://doi.org/10.1016/j.jas.2022.105695.

References

Albarède, F., Desaulty, A.M., Blichert-Toft, J., 2012. A geological perspective on the use of Pb isotopes in archaeometry. Archaeometry 54, 853–867. https://doi.org/10.1111/j.1475-4754.2011.00653.x.

Artioli, G., Canovaro, C., Nimis, P., Angelini, I., 2020. LIA of prehistoric metals in the central mediterranean area: a review. Archaeometry 62, 53–85. https://doi.org/10.1111/arcm.12542.

Aubert, D., Stille, P., Probst, A., 2001. REE fractionation during granite weathering and removal by waters and suspended loads: Sr and Nd isotopic evidence. Geochem. Cosmochim. Acta 65, 387–406. https://doi.org/10.1016/S0016-7037(00)00546-9.

Banner, J.L., 2004. Radiogenic isotopes: systematics and applications to earth surface processes and chemical stratigraphy. Earth Sci. Rev. 65, 141–194. https://doi.org/10.1016/S0012-8252(03)00086-2.

Barkoudah, Y., Henderson, J., 2006. Plant ashes from Syria and the manufacture of ancient glass: ethnographic and scientific aspects. J. Glass Stud. 297–321.

Bass, G.F., Lledo, B., Matthews, S., Brill, R.H., 2009. Serçe Limani. In: The Glass of an Eleventh-Century Shipwreck, vol. 2. Texas A&M University Press, College Station.

Bastian, L., Mologni, C., Vigier, N., Bayon, G., Lamb, H., Bosch, D., Kerros, M.E., Colin, C., Revel, M., 2021. Co-Variations of climate and silicate weathering in the nile basin during the late pleistocene. Quat. Sci. Rev. 264 https://doi.org/10.1016/j.quascirev.2021.107012.

Bataille, C.P., Bowen, G.J., 2012. Mapping 87Sr/86Sr variations in bedrock and water for large scale provenance studies. Chem. Geol. 304–305, 39–52. https://doi.org/10.1016/j.chemgeo.2012.01.028.

Bataille, C.P., Brennan, S.R., Hartmann, J., Moosdorf, N., Wooller, M.J., Bowen, G.J., 2014. A geostatistical framework for predicting variability in strontium concentrations and isotope ratios in Alaskan rivers. Chem. Geol. 389, 1–15. https://doi.org/10.1016/j.chemgeo.2014.08.030.

Bataille, C.P., Crowley, B.E., Wooller, M.J., Bowen, G.J., 2020. Advances in global bioavailable strontium isoscapes. Palaeogeogr. Palaeoclimatol. Palaeoecol. 555 https://doi.org/10.1016/j.palaeo.2020.109849.

Bataille, C.P., von Holstein, I.C.C., Laffoon, J.E., Willmes, M., Liu, X.M., Davies, G.R., 2018. A bioavailable strontium isoscape for Western Europe: a machine learning approach. PLoS One 13. https://doi.org/10.1371/journal.pone.0197386.

Bayon, G., Freslon, N., Germain, Y., Bindeman, I.N., Trinquier, A., Barrat, J.A., 2021. A global survey of radiogenic strontium isotopes in river sediments. Chem. Geol. 559 https://doi.org/10.1016/j.chemgeo.2020.119958.

Bayon, G., German, C.R., Boella, R.M., Milton, J.A., Taylor, R.N., Nesbitt, R.W., 2002. An improved method for extracting marine sediment fractions and its application to Sr and Nd isotopic analysis. Chem. Geol. 187, 179–199. https://doi.org/10.1016/S0009-2541(01)00416-8.

Bayon, G., Lambert, T., Vigier, N., De Deckker, P., Freslon, N., Jang, K., Larkin, C.S., Piotrowski, A.M., Tachikawa, K., Thollon, M., Tipper, E.T., 2020. Rare earth element and neodymium isotope tracing of sedimentary rock weathering. Chem. Geol. 553 https://doi.org/10.1016/j.chemgeo.2020.119794.

Bayon, G., Toucanne, S., Skonieczny, C., André, L., Bermell, S., Cheron, S., Dennielou, B., Etoubleau, J., Freslon, N., Gauchery, T., Germain, Y., Jorry, S.J., Ménot, G., Monin, L., Ponzevera, E., Rouget, M.L., Tachikawa, K., Barrat, J.A., 2015. Rare earth elements and neodymium isotopes in world river sediments revisited. Geochem. Cosmochim. Acta 170, 17–38. https://doi.org/10.1016/j.gca.2015.08.001.

Beard, B., Johnson, C., 2000. Strontium isotope composition of skeletal material can determine the birth place and geographic mobility of humans and animals. J. Forensic Sci. 45 https://doi.org/10.1520/jfs14829j.

Bentley, A.R., 2006. Strontium isotopes from the earth to the archaeological skeleton: a review. J. Archaeol. Method Theor 13, 135–187. https://doi.org/10.1007/s10816-006-9009-x.

Bialik, O.M., Frank, M., Betzler, C., Zammit, R., Waldmann, N.D., 2019. Two-step closure of the Miocene Indian ocean gateway to the mediterranean. Sci. Rep. 9 https://doi.org/10.1038/s41598-019-45308-7.

Blanchet, C.L., 2019. A database of marine and terrestrial radiogenic Nd and Sr isotopes for tracing earth-surface processes. Earth Syst. Sci. Data 11, 741–759. https://doi.org/10.5194/essd-11-741-2019.

Blank, M., Sjogren, K.G., Knipper, C., Frei, K.M., Stora, J., 2018. Isotope values of the bioavailable strontium in inland southwestern Sweden-A baseline for mobility studies. PLoS One 13. https://doi.org/10.1371/journal.pone.0204649.

Blum, J.D., Taliaferro, E.H., Weisse, M.T., Holmes, R.T., 2000. Changes in Sr/Ca, Ba/Ca and 87Sr/86Sr ratios between trophic levels in two forest ecosystems in the northeastern U.S.A. Biogeochemistry 49, 87–101. https://doi.org/10.1023/A:1006390707989.

Brems, D., Degryse, P., Hasendoncks, F., Gimeno, D., Silvestri, A., Vassilieva, E., Luypaers, S., Honings, J., 2012. Western Mediterranean sand deposits as a raw material for Roman glass production. J. Archaeol. Sci. 39, 2897–2907. https://doi.org/10.1016/j.jas.2012.03.009.

Brems, D., Ganio, M., Degryse, P., 2014. The Sr-Nd isotopic fingerprint of sand raw materials. In: Glass Making in the Greco-Roman World - Results of the ARCHGLASS Project. Leuven University Press, pp. 51–67.

Brems, D., Ganio, M., Latruwe, K., Balcaen, L., Carremans, M., Gimeno, D., Silvestri, A., Vanhaecke, F., Muchez, P., Degryse, P., 2013a. Isotopes On The Beach, Part 1: Strontium Isotope Ratios As A Provenance Indicator For Lime Raw Materials Used In Roman Glass-Making. Archaeometry 55, 214–234. https://doi.org/10.1111/j.1475-4754.2012.00702.x.

Brems, D., Ganio, M., Latruwe, K., Balcaen, L., Carremans, M., Gimeno, D., Silvestri, A., Vanhaecke, F., Muchez, P., Degryse, P., 2013b. Isotopes on the beach, part 2: Neodymium isotopic analysis for the provenancing of roman glass-making. Archaeometry 55, 449–464. https://doi.org/10.1111/j.1475-4754.2012.00701.x.

Brennan, S.R., Torgersen, C.E., Hollenbeck, J.P., Fernandez, D.P., Jensen, C.K., Schindler, D.E., 2016. Dendritic network models: Improving isoscapes and quantifying influence of landscape and in-stream processes on strontium isotopes in rivers. Geophys. Res. Lett. 43, 5043–5051. https://doi.org/10.1002/2016GL068904.

Brill, R.H., 1999. Tables of Analyses. In: Chemical Analyses of Early Glasses: Volume 2. Corning Museum of Glass, Corning.

Brill, R.H., Fullagar, P.D., 2009. Strontium-isotope studies of historical glasses and related materials: a progress report. In: Annales Du 17e Congres de l'Association Internationale Pour l'Histoire Du Verre - 2006. University Press Antwerp, pp. 552–557.

Bujakaite, M.I., Poleshchuk, A.V., Pokrovsky, B.G., 2016. Strontium, oxygen, and carbon isotope systems in the Quaternary loess sediments of Kirgizia. In: Proceedings of 21st Symposium on Isotope Geochemistry. Russia, Moscow, pp. 142–144.

Burke, W.H., Denison, R.E., Hetherington, E.A., Koepnick, R.B., Nelson, H.F., Otto, J., 1982. Variation of seawater 87Sr/86Sr through Phanerozoic time. Geology 10, 516–519.

Buzon, M.R., Simonetti, A., 2013. Strontium isotope (87Sr/86Sr) variability in the Nile Valley: Identifying residential mobility during ancient Egyptian and Nubian sociopolitical changes in the New Kingdom and Napatan periods. Am. J. Phys. Anthropol. 151, 1–9. https://doi.org/10.1002/ajpa.22235.

Capo, R.C., Chadwick, O.A., 1999. Sources of strontium and calcium in desert soil and calcrete. Earth Planet Sci. Lett. 170, 61–72. https://doi.org/10.1016/S0012-821X(99)00090-4.

Capo, R.C., Stewart, B.W., Chadwick, O.A., 1998. Strontium isotopes as tracers of ecosystem processes: Theory and methods. Geoderma 82, 197–225. https://doi.org/10.1016/S0016-7061(97)00102-X.

Carter, S.W., Wiegand, B., Mahood, G.A., Dudas, F.O., Wooden, J.L., Sullivan, A.P., Bowring, S.A., 2011. Strontium isotopic evidence for prehistoric transport of gray-ware ceramic materials in the eastern Grand Canyon region, USA. Geoarchaeology 26, 189–218. https://doi.org/10.1002/gea.20348.

Chen, J., Li, G., Yang, J., Rao, W., Lu, H., Balsam, W., Sun, Y., Ji, J., 2007. Nd and Sr isotopic characteristics of Chinese deserts: Implications for the provenances of Asian dust. Geochem. Cosmochim. Acta 71, 3904–3914. https://doi.org/10.1016/j.gca.2007.04.033.

Clauer, N., Chaudhuri, S., Toulkeridis, T., Blanc, G., 2000. Fluctuations of Caspian Sea level: Beyond climatic variations? Geology 28, 1015. https://doi.org/10.1130/0091-7613(2000)28<1015:focslb>2.0.co;2.

Cullen, H.M., deMenocal, P.B., Hemming, S., Hemming, G., Brown, F.H., Guilderson, T., Sirocko, F., 2000. Climate change and the collapse of the Akkadian empire: Evidence from the deep sea. Geology 28, 379–382. https://doi.org/10.1130/0091-7613(2000)28<379:CCATCO>2.0.CO;2.

De Bonis, A., Arienzo, I., D'Antonio, M., Franciosi, L., Germinario, C., Grifa, C., Guarino, V., Langella, A., Morra, V., 2018. Sr-Nd isotopic fingerprinting as a tool for ceramic provenance: Its application on raw materials, ceramic replicas and ancient pottery. J. Archaeol. Sci. 94, 51–59. https://doi.org/10.1016/j.jas.2018.04.002.

Degryse, P., Boyce, A., Erb-Satullo, N., Eremin, K., Kirk, S., Scott, R., Shortland, A.J., Schneider, J., Walton, M., 2010a. Isotopic discriminants between late bronze age glasses from egypt and the near east. Archaeometry 52, 380–388. https://doi.org/10.1111/j.1475-4754.2009.00487.x.

Degryse, P., Freestone, I.C., Schneider, J., Jennings, S., 2010b. Technology and provenance of Levantine plant ash glass using Sr-Nd isotope analysis. In: Glass in Byzantium - Production, Usage, Analyses. Römisch-Germanisches Zentralmuseum, pp. 83–90.

Degryse, P., Lobo, L., Shortland, A., Vanhaecke, F., Blomme, A., Painter, J., Gimeno, D., Eremin, K., Greene, J., Kirk, S., Walton, M., 2015. Isotopic investigation into the raw materials of Late Bronze Age glass making. J. Archaeol. Sci. 62, 153–160. https://doi.org/10.1016/j.jas.2015.08.004.

Degryse, P., Schneider, J., 2008. Pliny the Elder and Sr-Nd isotopes: tracing the provenance of raw materials for Roman glass production. J. Archaeol. Sci. 35, 1993–2000. https://doi.org/10.1016/j.jas.2008.01.002.

Degryse, P., Schneider, J., Haack, U., Lauwers, V., Poblome, J., Waelkens, M., Muchez, P., 2006. Evidence for glass "recycling" using Pb and Sr isotopic ratios and Sr-mixing lines: The case of early Byzantine Sagalassos. J. Archaeol. Sci. 33, 494–501. https://doi.org/10.1016/j.jas.2005.09.003.

Degryse, P., Shortland, A., De Muynck, D., Van Heghe, L., Scott, R., Neyt, B., Vanhaecke, F., 2010c. Considerations on the provenance determination of plant ash

glasses using strontium isotopes. J. Archaeol. Sci. 37, 3129–3135. https://doi.org/10.1016/j.jas.2010.07.014.
Dewan, N., Majestic, B.J., Ketterer, M.E., Miller-Schulze, J.P., Shafer, M.M., Schauer, J.J., Solomon, P.A., Artamonova, M., Chen, B.B., Imashev, S.A., Carmichael, G.R., 2015. Stable isotopes of lead and strontium as tracers of sources of airborne particulate matter in Kyrgyzstan. Atmos. Environ. 120, 438–446. https://doi.org/10.1016/j.atmosenv.2015.09.017.
Elliott, S., Bendrey, R., Whitlam, J., Aziz, K.R., Evans, J., 2015. Preliminary ethnoarchaeological research on modern animal husbandry in Bestansur, Iraqi Kurdistan: Integrating animal, plant and environmental data. Environ. Archaeol. 20, 283–303. https://doi.org/10.1179/1749631414Y.0000000025.
Ericson, J.E., 1985. Strontium Isotope Characterization in the Study of Prehistoric Human Ecology. J. Hum. Evol. 14, 503–514. https://doi.org/10.1016/S0047-2484(85)80029-4.
Evans, J.A., Montgomery, J., Wildman, G., 2009. Isotope domain mapping of 87Sr/86Sr biosphere variation on the Isle of Skye, Scotland. J. Geol. Soc. London. 166, 617–631. https://doi.org/10.1144/0016-76492008-043.
Evans, J.A., Montgomery, J., Wildman, G., Boulton, N., 2010. Spatial variations in biosphere 87Sr/86Sr in Britain. J. Geol. Soc. London 167, 1–4. https://doi.org/10.1144/0016-76492009-090.
Evans, J.A., Tatham, S., 2004. Defining "local signature" in terms of Sr isotope composition using a tenth- to twelfth-century Anglo-Saxon population living on a Jurassic clay-carbonate terrain, Rutland, UK. Geol. Soc. Spec. Publ. 232, 237–248. https://doi.org/10.1144/GSL.SP.2004.232.01.21.
Faure, G., Mensing, T.M., 2005. Isotopes: Principles and Applications. John Wiley & Sons, Inc.
Feng, J.L., Zhu, L.P., Zhen, X.L., Hu, Z.G., 2009. Grain size effect on Sr and Nd isotopic compositions in eolian dust: Implications for tracing dust provenance and Nd model age. Geochem. J. 43, 123–131. https://doi.org/10.2343/geochemj.1.0007.
Fiorentino, S., Venezia, B., Schibille, N., Vandini, M., 2019. Streams across the Silk Roads? The case of Islamic glass from Ghazni. J. Archaeol. Sci. Reports 25, 153–170. https://doi.org/10.1016/j.jasrep.2019.04.002.
Fouad, S.F., 2010. Tectonic and structural evolution of the Mesopotamia Foredeep, Iraq. Iraqi Bull. Geol. Min. 6, 41–53.
Frank, M., 2002. Radiogenic isotopes: Tracers of past ocean circulation and erosional input. Rev. Geophys. 40 (1) https://doi.org/10.1029/2000RG000094.
Freestone, I.C., 2006. Glass production in Late Antiquity and the Early Islamic period: A geochemical perspective. Geol. Soc. Spec. Publ. 257, 201–216. https://doi.org/10.1144/GSL.SP.2006.257.01.16.
Freestone, I.C., 2002. Composition and affinities of glass from the furnaces on the island site, Tyre. J. Glass Stud. 44, 67–77.
Freestone, I.C., Gorin-Rosen, Y., Hughes, M.J., 2000. Primary glass from Israel and the production of glass in late antiquity and the early Islamic period. Trav. la Maison l'Orient méditerranéen 65–88.
Freestone, I.C., Leslie, K.A., Thirlwall, M., Gorin-Rosen, Y., 2003. Strontium isotopes in the investigation of early glass production: Byzantine and early islamic glass from the near East. Archaeometry 45, 19–32. https://doi.org/10.1111/1475-4754.00094.
Frei, K.M., Frei, R., 2011. The geographic distribution of strontium isotopes in Danish surface waters - A base for provenance studies in archaeology, hydrology and agriculture. Appl. Geochem. 26, 326–340. https://doi.org/10.1016/j.apgeochem.2010.12.006.
Ganio, M., Boyen, S., Fenn, T., Scott, R., Vanhoutte, S., Gimeno, D., Degryse, P., 2012. Roman glass across the Empire: An elemental and isotopic characterization. J. Anal. At. Spectrom. 27, 743–753. https://doi.org/10.1039/c2ja10355a.
Ganio, M., Gulmini, M., Latruwe, K., Vanhaecke, F., Degryse, P., 2013. Sasanian glass from Veh Ardašīr investigated by strontium and neodymium isotopic analysis. J. Archaeol. Sci. 40, 4264–4270. https://doi.org/10.1016/j.jas.2013.06.018.
Gliozzo, E., Braschi, E., Langone, A., Ignelzi, A., Favia, P., Giuliani, R., 2021. New geochemical and Sr-Nd isotopic data on medieval plant ash-based glass: The glass collection from San Lorenzo in Carmignano (12th-14th centuries AD, Italy). Microchem. J. 168 https://doi.org/10.1016/j.microc.2021.106371.
Goldstein, S.J., Jacobsen, S.B., 1988. Nd and Sr isotopic systematics of river water suspended material: implications for crustal evolution. Earth Planet Sci. Lett. 87, 249–265. https://doi.org/10.1016/0012-821X(88)90013-1.
Goldstein, S.L., O'Nions, R.K., Hamilton, P.J., 1984. A Sm-Nd isotopic study of atmospheric dusts and particulates from major river systems. Earth Planet Sci. Lett. 70, 221–236. https://doi.org/10.1016/0012-821X(84)90007-4.
Gregoricka, L.A., 2014. Assessing life history from commingled assemblages: The biogeochemistry of inter-tooth variability in Bronze Age Arabia. J. Archaeol. Sci. 47, 10–21. https://doi.org/10.1016/j.jas.2014.04.004.
Gregoricka, L.A., 2013. Residential mobility and social identity in the periphery: Strontium isotope analysis of archaeological tooth enamel from southeastern Arabia. J. Archaeol. Sci. 40, 452–464. https://doi.org/10.1016/j.jas.2012.07.017.
Grousset, F.E., Biscaye, P.E., 2005. Tracing dust sources and transport patterns using Sr, Nd and Pb isotopes. Chem. Geol. 222, 149–167. https://doi.org/10.1016/j.chemgeo.2005.05.006.
Grousset, F.E., Parra, M., Bory, A., Martinez, P., Bertrand, P., Shimmield, G., Ellam, R.M., 1998. Saharan wind regimes traced by the Sr-Nd isotopic composition of subtropical Atlantic sediments: Last Glacial Maximum vs today. Quat. Sci. Rev. 17, 395–409. https://doi.org/10.1016/S0277-3791(97)00048-6.
Hartman, G., Richards, M., 2014. Mapping and defining sources of variability in bioavailable strontium isotope ratios in the Eastern Mediterranean. Geochem. Cosmochim. Acta 126, 250–264. https://doi.org/10.1016/j.gca.2013.11.015.
Hedman, K.M., Curry, B.B., Johnson, T.M., Fullagar, P.D., Emerson, T.E., 2009. Variation in strontium isotope ratios of archaeological fauna in the Midwestern United States: a preliminary study. J. Archaeol. Sci. 36, 64–73. https://doi.org/10.1016/j.jas.2008.07.009.
Hegg, J.C., Kennedy, B.P., Fremier, A.K., 2013. Predicting strontium isotope variation and fish location with bedrock geology: Understanding the effects of geologic heterogeneity. Chem. Geol. 360–361, 89–98. https://doi.org/10.1016/j.chemgeo.2013.10.010.
Henderson, J., Chenery, S., Faber, E., Kröger, J., 2016. The use of electron probe microanalysis and laser ablation-inductively coupled plasma-mass spectrometry for the investigation of 8th-14th century plant ash glasses from the Middle East. Microchem. J. 128, 134–152. https://doi.org/10.1016/j.microc.2016.03.013.
Henderson, J., Evans, J., Barkoudah, Y., 2009. The roots of provenance: glass, plants and isotopes in the islamic middle east. Antiquity 83, 414–429. https://doi.org/10.1017/S0003598X00098525.
Henderson, J., Evans, J., Bellintani, P., Bietti-Sestieri, A.M., 2015. Production, mixing and provenance of Late Bronze Age mixed alkali glasses from northern Italy: An isotopic approach. J. Archaeol. Sci. 55, 1–8. https://doi.org/10.1016/j.jas.2014.12.006.
Henderson, J., Evans, J., Nikita, K., 2010. Isotopic evidence for the primary production, provenance and trade of late bronze age glass in the mediterranean. Mediterr. Archaeol. Archaeom. 10, 1–24.
Henderson, J., Evans, J.A., Sloane, H.J., Leng, M.J., Doherty, C., 2005. The use of oxygen, strontium and lead isotopes to provenance ancient glasses in the Middle East. J. Archaeol. Sci. 32, 665–673. https://doi.org/10.1016/j.jas.2004.05.008.
Henderson, J., Ma, H., Cui, J., Ma, R., Xiao, H., 2020a. Isotopic investigations of Chinese ceramics. Archaeol. Anthropol. Sci. 12 https://doi.org/10.1007/s12520-020-01138-7.
Henderson, J., Ma, H., Evans, J., 2020b. Glass production for the Silk Road? Provenance and trade of islamic glasses using isotopic and chemical analyses in a geological context. J. Archaeol. Sci. 119 https://doi.org/10.1016/j.jas.2020.105164.
Henderson, J., McLoughlin, S.D., McPhail, D.S., 2004. Radical changes in Islamic glass technology: Evidence for conservatism and experimentation with new glass recipes from early and middle Islamic Raqqa, Syria. Archaeometry 46, 439–468. https://doi.org/10.1111/j.1475-4754.2004.00167.x.
Hindshaw, R.S., Aciego, S.M., Piotrowski, A.M., Tipper, E.T., 2018. Decoupling of dissolved and bedrock neodymium isotopes during sedimentary cycling. Geochemical Perspect. Lett. 8, 43–46. https://doi.org/10.7185/geochemlet.1828.
Hodell, D.A., Quinn, R.L., Brenner, M., Kamenov, G., 2004. Spatial variation of strontium isotopes (87Sr/86Sr) in the Maya region: A tool for tracking ancient human migration. J. Archaeol. Sci. 31, 585–601. https://doi.org/10.1016/j.jas.2003.10.009.
Hodos, T., Cartwright, C.R., Montgomery, J., Nowell, G., Crowder, K., Fletcher, A.C., Gönster, Y., 2020. The origins of decorated ostrich eggs in the ancient Mediterranean and Middle East. Antiquity 94, 381–400. https://doi.org/10.15184/aqy.2020.14.
Holt, E., Evans, J.A., Madgwick, R., 2021. Strontium (87Sr/86Sr) mapping: A critical review of methods and approaches. Earth Sci. Rev. 216 https://doi.org/10.1016/j.earscirev.2021.103593.
Hoppe, K.A., Koch, P.L., Furutani, T.T., 2003. Assessing the preservation of biogenic strontium in fossil bones and tooth enamel. Int. J. Osteoarchaeol. 13, 20–28. https://doi.org/10.1002/oa.663.
Jacobsen, S.B., Wasserburg, G.J., 1980. Sm-Nd isotopic evolution of chondrites. Earth Planet Sci. Lett. 50, 139–155. https://doi.org/10.1016/0012-821X(80)90125-9.
James, H.F., Adams, S., Willmes, M., Mathison, K., Ulrichsen, A., Wood, R., Valera, A.C., Frieman, C.J., Grün, R., 2022. A large-scale environmental strontium isotope baseline map of Portugal for archaeological and paleoecological provenance studies. J. Archaeol. Sci. 142, 105595 https://doi.org/10.1016/j.jas.2022.105595.
Janzen, A., Bataille, C., Copeland, S.R., Quinn, R.L., Ambrose, S.H., Reed, D., Hamilton, M., Grimes, V., Richards, M.P., le Roux, P., Roberts, P., 2020. Spatial variation in bioavailable strontium isotope ratios (87Sr/86Sr) in Kenya and northern Tanzania: Implications for ecology, paleoanthropology, and archaeology. Palaeogeogr. Palaeoclimatol. Palaeoecol. 560, 109957 https://doi.org/10.1016/j.palaeo.2020.109957.
Jeandel, C., Arsouze, T., Lacan, F., Téchiné, P., Dutay, J.C., 2007. Isotopic Nd compositions and concentrations of the lithogenic inputs into the ocean: A compilation, with an emphasis on the margins. Chem. Geol. 239, 156–164. https://doi.org/10.1016/j.chemgeo.2006.11.013.
Kenoyer, J.M., Price, T.D., Burton, J.H., 2013. A new approach to tracking connections between the Indus Valley and Mesopotamia: Initial results of strontium isotope analyses from Harappa and Ur. J. Archaeol. Sci. 40, 2286–2297. https://doi.org/10.1016/j.jas.2012.12.040.
Khademi, H., Mermut, A.R., Krouse, H.R., 1997. Sulfur isotope geochemistry of gypsiferous Aridisols from central Iran. Geoderma 80, 195–209. https://doi.org/10.1016/S0016-7061(97)00091-8.
Khormali, F., Toomanian, N., 2018. Soil-Forming Factors and Processes. In: The Soils of Iran. Springer, pp. 73–91. https://doi.org/10.1007/978-3-319-69048-3_6.
Killick, D.J., Stephens, J.A., Fenn, T.R., 2020. Geological constraints on the use of lead isotopes for provenance in archaeometallurgy. Archaeometry 62, 86–105. https://doi.org/10.1111/arcm.12573.
Knudson, K.J., Price, T.D., 2007. Utility of multiple chemical techniques in archaeological residential mobility studies: Case studies from Tiwanaku- and Chiribaya-affiliated sites in the Andes. Am. J. Phys. Anthropol. 132, 25–39. https://doi.org/10.1002/ajpa.20480.
Koch, P.L., Tuross, N., Fogel, M.L., 1997. The Effects of Sample Treatment and Diagenesis on the Isotopic Integrity of Carbonate in Biogenic Hydroxylapatite. J. Archaeol. Sci. 24, 417–429. https://doi.org/10.1006/jasc.1996.0126.
Kröger, J., 1995. Nishapur: Glass of the Early Islamic Period. The Metropolitan Museum of Art, New York.

Kumar, A., Suresh, K., Rahaman, W., 2020. Geochemical characterization of modern aeolian dust over the Northeastern Arabian Sea: Implication for dust transport in the Arabian Sea. Sci. Total Environ. 729 https://doi.org/10.1016/j.scitotenv.2020.138576.

Kutterer, A., Uerpmann, H.P., 2017. Neolithic nomadism in south-east Arabia — strontium and oxygen isotope ratios in human tooth enamel from al-Buhais 18 and Umm al-Quwain 2 in the Emirates of Sharjah and Umm al-Quwain (UAE). Arabian Archaeol. Epigr. 28, 75–89. https://doi.org/10.1111/aae.12084.

Lacan, F., Tachikawa, K., Jeandel, C., 2012. Neodymium isotopic composition of the oceans: A compilation of seawater data. Chem. Geol. 300–301, 177–184. https://doi.org/10.1016/j.chemgeo.2012.01.019.

Ladegaard-Pedersen, P., Achilleos, M., Dörflinger, G., Frei, R., Kristiansen, K., Frei, K.M., 2020. A strontium isotope baseline of Cyprus. Assessing the use of soil leachates, plants, groundwater and surface water as proxies for the local range of bioavailable strontium isotope composition. Sci. Total Environ. 708 https://doi.org/10.1016/j.scitotenv.2019.134714.

Laffoon, J.E., Davies, G.R., Hoogland, M.L.P., Hofman, C.L., 2012. Spatial variation of biologically available strontium isotopes (87Sr/86Sr) in an archipelagic setting: A case study from the Caribbean. J. Archaeol. Sci. 39, 2371–2384. https://doi.org/10.1016/j.jas.2012.02.002.

Lengfelder, F., Grupe, G., Stallauer, A., Huth, R., Söllner, F., 2019. Modelling strontium isotopes in past biospheres – Assessment of bioavailable 87Sr/86Sr ratios in local archaeological vertebrates based on environmental signatures. Sci. Total Environ. 648, 236–252. https://doi.org/10.1016/j.scitotenv.2018.08.014.

Li, B.P., Zhao, J.X., Greig, A., Collerson, K.D., Feng, Y.X., Sun, X.M., Guo, M. Sen, Zhou, Z.X., 2006. Characterisation of Chinese Tang sancai from Gongxian and Yaozhou kilns using ICP-MS trace element and TIMS Sr-Nd isotopic analysis. J. Archaeol. Sci. 33, 56–62. https://doi.org/10.1016/j.jas.2005.06.007.

Li, B.P., Zhao, J.X., Greig, A., Collerson, K.D., Zhuo, Z.X., Feng, Y.X., 2005. Potential of Sr isotopic analysis in ceramic provenance studies: Characterisation of Chinese stonewares. Nucl. Instrum. Methods Phys. Res. Sect. B Beam Interact. Mater. Atoms 240, 726–732. https://doi.org/10.1016/j.nimb.2005.06.003.

Li, G., Pettke, T., Chen, J., 2011. Increasing Nd isotopic ratio of Asian dust indicates progressive uplift of the north Tibetan Plateau since the middle Miocene. Geology 39, 199–202. https://doi.org/10.1130/G31734.1.

Li, Y., Song, Y., Fitzsimmons, K.E., Chen, X., Wang, Q., Sun, H., Zhang, Z., 2018. New evidence for the provenance and formation of loess deposits in the Ili River Basin, Arid Central Asia. Aeolian Res 35, 1–8. https://doi.org/10.1016/j.aeolia.2018.08.002.

Lü, Q.-Q., Henderson, J., Wang, Y., Wang, B., 2021. Natron glass beads reveal proto-Silk Road between the Mediterranean and China in the 1st millennium BCE. Sci. Rep. 11 https://doi.org/10.1038/s41598-021-82245-w.

Maurer, A.F., Galer, S.J.G., Knipper, C., Beierlein, L., Nunn, E.V., Peters, D., Tütken, T., Alt, K.W., Schöne, B.R., 2012. Bioavailable 87Sr/86Sr in different environmental samples - Effects of anthropogenic contamination and implications for isoscapes in past migration studies. Sci. Total Environ. 216–229. https://doi.org/10.1016/j.scitotenv.2012.06.046.

McArthur, J.M., Howarth, R.J., Shields, G.A., 2012. Strontium isotope stratigraphy. In: The Geologic Time Scale 2012, pp. 127–144. https://doi.org/10.1016/B978-0-444-59425-9.00007-X.

Meyer, I., Davies, G.R., Stuut, J.B.W., 2011. Grain size control on Sr-Nd isotope provenance studies and impact on paleoclimate reconstructions: An example from deep-sea sediments offshore NW Africa. Geochem. Geophys. Geosy. 12 https://doi.org/10.1029/2010GC003355.

Mirti, P., Pace, M., Malandrino, M., Ponzi, M.N., 2009. Sasanian glass from Veh Ardaš̄ır: new evidences by ICP-MS analysis. J. Archaeol. Sci. 36, 1061–1069. https://doi.org/10.1016/j.jas.2008.12.008.

Mirti, P., Pace, M., Negro Ponzi, M.M., Aceto, M., 2008. ICP-MS analysis of glass fragments of Parthian and Sasanian epoch from Seleucia and Veh Ardaš̄ır (Central Iraq). Archaeometry 50, 429–450. https://doi.org/10.1111/j.1475-4754.2007.00344.x.

Mokadem, F., Parkinson, I.J., Hathorne, E.C., Anand, P., Allen, J.T., Burton, K.W., 2015. High-precision radiogenic strontium isotope measurements of the modern and glacial ocean: Limits on glacial-interglacial variations in continental weathering. Earth Planet Sci. Lett. 415, 111–120. https://doi.org/10.1016/j.epsl.2015.01.036.

Montgomery, J., Evans, J.A., Cooper, R.E., 2007. Resolving archaeological populations with Sr-isotope mixing models. Appl. Geochem. 22, 1502–1514. https://doi.org/10.1016/j.apgeochem.2007.02.009.

Nafplioti, A., 2011. Tracing population mobility in the Aegean using isotope geochemistry: A first map of local biologically available 87Sr/86Sr signatures. J. Archaeol. Sci. 38, 1560–1570. https://doi.org/10.1016/j.jas.2011.02.021.

Nagatsuka, N., Takeuchi, N., Nakano, T., Shin, K., Kokado, E., 2014. Geographical variations in Sr and Nd isotopic ratios of cryoconite on Asian glaciers. Environ. Res. Lett. 9 https://doi.org/10.1088/1748-9326/9/4/045007.

Pernicka, E., 2013. Provenance determination of archaeological metal objects. Archaeometall. Glob. Perspect. Methods Synth. 239–268. https://doi.org/10.1007/978-1-4614-9017-3_11.

Pett-Ridge, J.C., Derry, L.A., Kurtz, A.C., 2009. Sr isotopes as a tracer of weathering processes and dust inputs in a tropical granitoid watershed, Luquillo Mountains, Puerto Rico. Geochem. Cosmochim. Acta 73, 25–43. https://doi.org/10.1016/j.gca.2008.09.032.

Phelps, M., 2018. Glass supply and trade in early Islamic Ramla: an investigation of the plant ash glass. In: Things that Travelled: Mediterranean Glass in the First Millennium CE. UCL Press, pp. 236–282.

Pokrovsky, B.G., Zaviyalov, P.O., Bujakaite, M.I., Izhitskiy, A.S., Petrov, O.L., Kurbaniyazov, A.K., Shimanovich, V.M., 2017. Geochemistry of O, H, C, S, and Sr isotopes in the water and sediments of the Aral basin. Geochem. Int. 55, 1033–1045. https://doi.org/10.1134/S0016702917110076.

Pollard, A.M., Bray, P.J., 2015. A New Method For Combining Lead Isotope and Lead Abundance Data to Characterize Archaeological Copper Alloys. Archaeometry 57, 996–1008. https://doi.org/10.1111/arcm.12145.

Posey, R.G., 2011. Development and Validation of a Spatial Prediction Model for Forensic Geographical Provenancing of Human Remains. University of East Anglia.

Poszwa, A., Ferry, B., Dambrine, E., Pollier, B., Wickman, T., Loubet, M., Bishop, K., 2004. Variations of bioavailable Sr concentration and 87Sr/86Sr ratio in boreal forest ecosystems. Biogeochemistry 67, 1–20. https://doi.org/10.1023/b:biog.0000015162.12857.3e.

Price, T.D., Burton, J.H., Bentley, R.A., 2002. The characterization of biologically available strontium isotope ratios for the study of prehistoric migration. Archaeometry 44, 117–135. https://doi.org/10.1111/1475-4754.00047.

Price, T.D., Johnson, C.M., Ezzo, J.A., Ericson, J., Burton, J.H., 1994. Residential mobility in the prehistoric southwest United States: A preliminary study using strontium isotope analysis. J. Archaeol. Sci. 21, 315–330. https://doi.org/10.1006/jasc.1994.1031.

Rehren, T., Freestone, I.C., 2015. Ancient glass: from kaleidoscope to crystal ball. J. Archaeol. Sci. 56, 233–241. https://doi.org/10.1016/j.jas.2015.02.021.

Rehren, T., Osorio, A., Anarbaev, A., 2010. Some notes on the early Islamic glass in Eastern Uzbekistan. In: Glass along the Silk Road from 200 BC to AD 1000. Römisch-Germanisches Zentralmuseum, pp. 93–103.

Robinson, S., Ivanovic, R., van de Flierdt, T., Blanchet, C.L., Tachikawa, K., Martin, E.E., Cook, C.P., Williams, T., Gregoire, L., Plancherel, Y., Jeandel, C., Arsouze, T., 2021. Global continental and marine detrital εNd: An updated compilation for use in understanding marine Nd cycling. Chem. Geol. 567, 120119 https://doi.org/10.1016/j.chemgeo.2021.120119.

Roozitalab, M.H., Toomanian, N., Dehkordi, V.R.G., Khormali, F., 2018. Major Soils, Properties, and Classification. In: The Soils of Iran, pp. 93–147. https://doi.org/10.1007/978-3-319-69048-3_7.

Ryan, S.E., Snoeck, C., Crowley, Q.G., Babechuk, M.G., 2018. 87Sr/86Sr and trace element mapping of geosphere-hydrosphere-biosphere interactions: A case study in Ireland. Appl. Geochem. 92, 209–224. https://doi.org/10.1016/j.apgeochem.2018.01.007.

Scaffidi, B.K., Knudson, K.J., 2020. An archaeological strontium isoscape for the prehistoric Andes: Understanding population mobility through a geostatistical meta-analysis of archaeological 87Sr/86Sr values from humans, animals, and artifacts. J. Archaeol. Sci. 117 https://doi.org/10.1016/j.jas.2020.105121.

Schibille, N., Gratuze, B., Ollivier, E., Blondeau, É., 2019. Chronology of early Islamic glass compositions from Egypt. J. Archaeol. Sci. 104, 10–18. https://doi.org/10.1016/j.jas.2019.02.001.

Schibille, N., Meek, A., Wypyski, M.T., Kröger, J., Rosser-Owen, M., Haddon, R.W., 2018. The glass walls of Samarra (Iraq): Ninth-century Abbasid glass production and imports. PLoS One 13. https://doi.org/10.1371/journal.pone.0201749.

Serna, A., Prates, L., Mange, E., Salazar-García, D.C., Bataille, C.P., 2020. Implications for paleomobility studies of the effects of quaternary volcanism on bioavailable strontium: A test case in North Patagonia (Argentina). J. Archaeol. Sci. 121, 105198 https://doi.org/10.1016/j.jas.2020.105198.

Sharifi, A., Murphy, L.N., Pourmand, A., Clement, A.C., Canuel, E.A., Naderi Beni, A., A. K. Lahijani, H., Delanghe, D., Ahmady-Birgani, H., 2018. Early-Holocene greening of the Afro-Asian dust belt changed sources of mineral dust in West Asia. Earth Planet Sci. Lett. 481, 30–40. https://doi.org/10.1016/j.epsl.2017.10.001.

Sillen, A., Hall, G., Richardson, S., Armstrong, R., 1998. 87Sr/86Sr ratios in modern and fossil food-webs of the Sterkfontein Valley: Implications for early hominid habitat preference. Geochem. Cosmochim. Acta 62, 2463–2473. https://doi.org/10.1016/S0016-7037(98)00182-3.

Sirocko, F., 1994. Abrupt Change in Monsoonal Climate: Evidence from the Geochemical Composition of Arabian Sea Sediments. Christian-Albrechts-Universität zu Kiel.

Snoeck, C., Ryan, S., Pouncett, J., Pellegrini, M., Claeys, P., Wainwright, A.N., Mattielli, N., Lee-Thorp, J.A., Schulting, R.J., 2020. Towards a biologically available strontium isotope baseline for Ireland. Sci. Total Environ. 712 https://doi.org/10.1016/j.scitotenv.2019.136248.

Stanley, J.D., Krom, M.D., Cliff, R.A., Woodward, J.C., 2003. Short contribution: Nile flow failure at the end of the Old Kingdom, Egypt: Strontium isotopic and petrologic evidence. Geoarchaeology 18, 395–402. https://doi.org/10.1002/gea.10065.

Stantis, C., Nowell, G.M., Prell, S., Schutkowski, H., 2019. Animal proxies to characterize the strontium biosphere in the Northeastern Nile Delta. Bioarchaeol. Near East 13, 1–13.

Stow, D., Nicholson, U., Kearsey, S., Tatum, D., Gardiner, A., Ghabra, A., Jaweesh, M., 2020. The Pliocene-Recent Euphrates river system: Sediment facies and architecture as an analogue for subsurface reservoirs. Energy Geosci 1, 174–193. https://doi.org/10.1016/j.engeos.2020.07.005.

Tachikawa, K., Arsouze, T., Bayon, G., Bory, A., Colin, C., Dutay, J.C., Frank, N., Giraud, X., Gourlan, A.T., Jeandel, C., Lacan, F., Meynadier, L., Montagna, P., Piotrowski, A.M., Plancherel, Y., Pucéat, E., Roy-Barman, M., Waelbroeck, C., 2017. The large-scale evolution of neodymium isotopic composition in the global modern and Holocene ocean revealed from seawater and archive data. Chem. Geol. 457, 131–148. https://doi.org/10.1016/j.chemgeo.2017.03.018.

Toomanian, N., Jalalian, A., Eghbal, M.K., 2001. Genesis of gypsum enriched soils in north-west Isfahan, Iran. Geoderma 99, 199–224. https://doi.org/10.1016/S0016-7061(00)00058-6.

Tudryn, A., Leroy, S.A.G., Toucanne, S., Gibert-Brunet, E., Tucholka, P., Lavrushin, Y.A., Dufaure, O., Miska, S., Bayon, G., 2016. The Ponto-Caspian basin as a final trap for southeastern Scandinavian Ice-Sheet meltwater. Quat. Sci. Rev. 148, 29–43. https://doi.org/10.1016/j.quascirev.2016.06.019.

Van Ham-Meert, A., Claeys, P., Jasim, S., Overlaet, B., Yousif, E., Degryse, P., 2019. Plant ash glass from first century CE Dibba. U.A.E. Archaeol. Anthropol. Sci. 11, 1431–1441. https://doi.org/10.1007/s12520-018-0611-0.

Voerkelius, S., Lorenz, G.D., Rummel, S., Quétel, C.R., Heiss, G., Baxter, M., Brach-Papa, C., Deters-Itzelsberger, P., Hoelzl, S., Hoogewerff, J., Ponzevera, E., Van Bocxstaele, M., Ueckermann, H., 2010. Strontium isotopic signatures of natural mineral waters, the reference to a simple geological map and its potential for authentication of food. Food Chem. 118, 933–940. https://doi.org/10.1016/j.foodchem.2009.04.125.

Walton, M., Eremin, K., Shortland, A., Degryse, P., Kirk, S., 2012. Analysis of Late Bronze Age glass axes from Nippur—a new cobalt colourant. Archaeometry 54, 835–852. https://doi.org/10.1111/j.1475-4754.2012.00664.x.

Wang, X., Tang, Z., 2020. The first large-scale bioavailable Sr isotope map of China and its implication for provenance studies. Earth Sci. Rev. 210 https://doi.org/10.1016/j.earscirev.2020.103353.

Wang, X., Tang, Z., Dong, X., 2018. Distribution of strontium isotopes in river waters across the tarim basin: A map for migration studies. J. Geol. Soc. London. 175, 967–973. https://doi.org/10.1144/jgs2018-074.

Wedepohl, K.H., Baumann, A., 2000. The use of marine molluskan shells for roman glass and local raw glass production in the Eifel area (western Germany). Naturwissenschaften 87, 129–132. https://doi.org/10.1007/s001140050690.

Weldeab, S., Emeis, K.C., Hemleben, C., Siebel, W., 2002. Provenance of lithogenic surface sediments and pathways of riverine suspended matter in the Eastern Mediterranean Sea: Evidence from 143Nd/144Nd and 87Sr/86Sr ratios. Chem. Geol. 186, 139–149. https://doi.org/10.1016/S0009-2541(01)00415-6.

White, W.M., Hofmann, A.W., 1982. Sr and Nd isotope geochemistry of oceanic basalts and mantle evolution. Nature 296, 821–825. https://doi.org/10.1038/296821a0.

Willmes, M., Bataille, C.P., James, H.F., Moffat, I., McMorrow, L., Kinsley, L., Armstrong, R.A., Eggins, S., Grün, R., 2018. Mapping of bioavailable strontium isotope ratios in France for archaeological provenance studies. Appl. Geochem. 90, 75–86. https://doi.org/10.1016/j.apgeochem.2017.12.025.

Willmes, M., McMorrow, L., Kinsley, L., Armstrong, R., Aubert, M., Eggins, S., Falguères, C., Maureille, B., Moffat, I., Grün, R., 2014. The IRHUM (Isotopic Reconstruction of Human Migration) database - Bioavailable strontium isotope ratios for geochemical fingerprinting in France. Earth Syst. Sci. Data 6, 117–122. https://doi.org/10.5194/essd-6-117-2014.

Woodward, J., Macklin, M., Fielding, L., Millar, I., Spencer, N., Welsby, D., Williams, M., 2015. Shifting sediment sources in the world's longest river: A strontium isotope record for the Holocene Nile. Quat. Sci. Rev. 130, 124–140. https://doi.org/10.1016/j.quascirev.2015.10.040.

Wu, X., Zhang, X., 2022. Discussion on several issues of Sr isotopic archaeology. Acta Anthropol. Sin. 41, 535–550. https://doi.org/10.16359/j.1000-3193/AAS.2021.0053.

Yacoub, S.Y., 2011. Stratigraphy of the mesopotamia plain. Iraqi Bull. Geol. Min. (4), 47–82.

Zhang, X., Chen, J., Ma, L., He, J., Wang, C., Qiu, P., 2004. Pb and Sr isotopic compositions of ancient pottery: a method to discriminate production sites. He Jishu/Nuclear Tech. 27, 201.